Maleic Anhydride Modified Oligo(isobutylene): Effect of Hydrogen Bonding on Its Associative Strength in Hexane Characterized by Fluorescence Spectroscopy

Anna K. Mathew and Jean Duhamel*

Department of Chemistry and Biochemistry, Institute for Polymer Research, University of Waterloo, Waterloo, ON N2L 3G1, Canada

Jason Gao

Imperial Oil Research Department, P.O. 3022, Sarnia, ON N7T 8C8, Canada

Received July 12, 2000; Revised Manuscript Received December 4, 2000

ABSTRACT: The intermolecular associations of an oligoisobutylene with a maleic anhydride (MA) function at one of its ends were investigated in hexane by carefully monitoring the fluorescence response of a pyrene dye attached onto the MA moiety via an imide bond. Two pyrene-to-MA linkers were used. One consisted of a single methylene unit, and the other of an amide bond followed by three methylene units. Comparison of the fluorescence data obtained with the two pyrene-labeled oligoisobutylenes showed that very strong polar associations are obtained in hexane between modified oligoisobutylenes displaying an amide bond. The fluorescence decays were analyzed in a quantitative manner using two models, which yield the fraction of associated polar ends. Above an oligomer concentration of 40 g/L, more than 95% of the polar ends of the modified oligoisobutylenes displaying an amide bond are associated in hexane compared to less than 60% of the polar ends of the oligomer displaying no amide bond. In an apolar solvent, the amide bond can share its hydrogen with other imide moieties via an intermolecular process, which favors association. In more polar tetrahydrofuran, only 21% of the polar ends of both OIB−Pys are associated. These associations occur intramolecularly and are due to OIB chains displaying more than one MA moiety.

Introduction

Associating polymers (AP) are made of a solvent-soluble backbone onto which insoluble blocks have been grafted.[1] In the appropriate solvent, the polymer backbone is soluble and the insoluble moieties aggregate, an entropy-driven process which leads to the formation of large polymeric aggregates. These large structures yield very viscous solutions, even at low AP concentrations.[2] If a strong enough physical stress such as shear is applied to the AP solution, the aggregates dissociate, and the solution's viscosity drops.[3] The solution is said to undergo shear-thinning. These shear-induced viscoelastic properties have found numerous practical applications for APs. APs are used as viscosity modifiers in oils, thickeners in paints, colloidal stabilizers in oils and paints, and oil-recovery agents.[1]

Numerous studies have suggested that the peculiar viscoelastic properties of APs are the result of a subtle balance of intra- and intermolecular associations created between the associative pendants.[4] On the basis of rheological observations, models have been developed, which characterize APs viscoelastic behavior by assuming the presence of various entities in the AP solution.[5] These entities include bridges (an AP chain shares its associating pendants with other AP chains generating intermolecular connections), close micelles (an AP chain pools all its associating pendants into a single aggregate of associating pendants), or free (unassociated) pendants. Whereas rheology-based models make educated guesses about the fractions of associating moieties either involved into a bridge or a close micelle, or acting as an unassociated pendant, fluorescence spectroscopy can investigate some of these entities in an independent and direct manner.

Scheme 1. Birks' Model for Excimer Formation

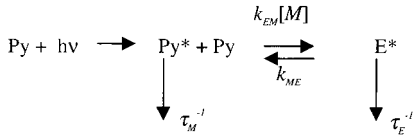

In this paper, we have used the ability of the dye pyrene to form an excimer in order to study a simple associating polymer and quantify the fraction of its associating groups involved into aggregates and the fraction of its associating groups, which were not aggregated. Pyrene is an often chosen dye to characterize polymer−polymer associations because the excimer formation process is usually well described by the classic Birks' scheme (cf. Scheme 1).[6] In Birks' scheme, an excited pyrene can either emit a photon with its own lifetime (τ_M), or encounter a ground-state pyrene via diffusion with a rate constant k_{EM} and form a complex called an excimer. The excimer can either fluoresce with a lifetime (τ_E) or dissociate with a dissociation rate constant k_{ME}. By monitoring the process of excimer formation between two pyrene groups attached onto an AP's associative pendants, qualitative information about the nature of AP's associations can be retrieved for either synthetic[7] or natural[8] polymers. However very few reports aim at using the information contained in the fluorescence data in a more quantitative manner. This is due to the very complex nature of these polymeric systems, which are often poorly defined in terms of molecular weight distribution and location of the

* To whom correspondence should be addressed.

10.1021/ma001211r CCC: $20.00
Published on Web 01/27/2001

Scheme 2. Oligo(isobutylene) Labelled with PMA (I) and PHZ (II) ($n \sim 50$)

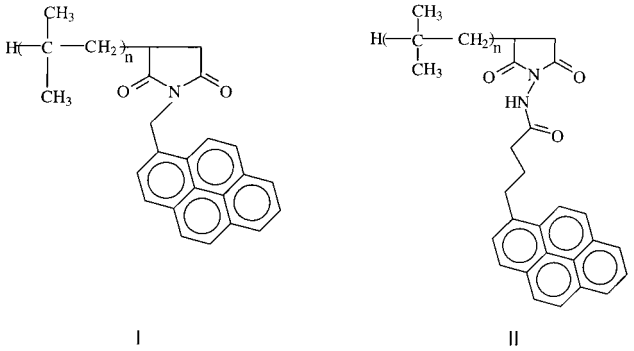

I II

associating pendants. In many AP systems, pendants are often randomly distributed along the polymer backbone.[1] The distribution of distances between pendants generates a distribution of rate constants k_{EM}, so that the process of excimer formation cannot be described by Scheme 1.[9] Furthermore, the associations existing between associated pyrenes induce the formation of ground-state pyrene dimers, which further complicates the analysis of the fluorescence data.[10] As a result, the classic Birks' scheme, which is the standard model for studying excimer formation, cannot be applied for pyrene-labeled APs.

The present work focuses on the associative properties in hexane of an oligoisobutylene at one end of which a single MA moiety has been attached (OIB−MA). When reacted with an amine-containing molecule, these modified oligomers are used as oil additives. Their polar moieties readily adsorb onto polar particulate matter, which is generated in the oil during the working of an engine, while their apolar tails stabilize the whole assembly.[11] The major feature of these modified oligoisobutylenes is their ability to associate strongly in apolar solvents via their polar moieties. Understanding how modifications made to a given oligoisobutylene do affect its associative strength would be very useful to design modified polymers with improved associative strength. We set out to answering these questions by studying the associative strength of modified oligoisobutylenes by fluorescence. Pyrene was attached onto the MA moieties using two linkers as shown in Scheme 2 to yield OIB−MA labeled with pyrene (OIB−Py). OIB−MA was labeled with 1-pyrenemethylamine (PMA) to yield OIB−PMA (**I**) and with 1-pyrenebutanoicacid hydrazide (PHZ) to yield OIB−PHZ (**II**). PMA and PHZ have been used in different studies to monitor the associative behavior in hexane of different polyolefins grafted with MA units.[12,13] However it is the first time that the associative strength of a PMA-labeled polymer is directly compared in the same report with that of a PHZ-labeled polymer. The different natures of the polymer-to-pyrene linker are expected to affect the strength of the associations between OIB−Pys in an apolar solvent. Labeling of OIB−MA with PMA yields a linker with one methylene unit, which is expected to be inert in an apolar solvent like hexane. Labeling of OIB−MA with PHZ yields a linker with three methylene units and an amide bond (−NH−CO−). The amide bond is expected to be rather polar in hexane and to enhance the associative ability of OIB−MA by generating hydrogen bonds. Of particular interest will be whether such small differences in the pyrene-to−polymer linker between the two otherwise identical molecules OIB−PMA and OIB−PHZ can have any effect on their associative strength.

One complication, which often arises when trying to determine the associative strength of modified polyolefins, is due to the MA grafting reaction. It is common knowledge that MA units often attach themselves as oligoMA onto polyolefins.[14] In turn oligoMA yields MA units, which are very close to one another, falsely suggesting that intermolecular association is occurring. Even at an extremely low oligomer concentration of the modified polyolefin where no intermolecular associations are possible, residual associations between MA groups seem to occur due to the presence of oligoMA. To determine whether associations between MA moieties are taking place intra- or intermolecularly, a thorough characterization of the oligomer microstructure is required in order to determine the fraction of MA involved into oligoMA grafts.

First the characterization of the OIB−MA microstructure was carried out by using fluorescence spectroscopy in THF, a polar solvent where associations between MA moieties are not favored.[12,13] Then the associative strength of the modified oligoisobutylenes is evaluated by determining the fractions of MA units, which are either associated or not associated. Understanding how the fraction of associated MA units does evolve for the two OIB−Pys when the solvent is switched from polar THF to apolar hexane constitutes the focus of the present article.

Experimental Section

Materials. The solvents THF (Caledon, distilled in glass), hexane (Fisher scientific, HPLC Grade), dodecane (Aldrich, 99%), toluene (EM Science, analytical reagent), xylene (BDH, analytical reagent), and acetone (BDH, Spectro Grade) were used as received. Trimethylsilyl diazomethane (2.0 M solution in hexanes) was purchased from Aldrich. OIB−MA was obtained from Imperial Oil. Pyrene methylamine hydrochloride (95%) was obtained from Aldrich. Pyrene butanoic acid hydrazide (95%) was purchased from Molecular Probes. Hexane (Fisher scientific, HPLC Grade) was freshly distilled over calcium hydride before preparing any oligomer solution.

Polymer Purification before Pyrene Labeling. The polymer was dissolved in hexane and precipitated by adding acetone. This process was repeated three times, and the precipitated polymer was dried under vacuum. This operation ensured that the polymer samples did not contain any ungrafted material before the pyrene labeling reaction.

Labeling of OIB with PMA. PMA was obtained from 1-pyrenylmethylamine hydrochloride as reported elsewhere.[15] After neutralization, PMA in hexane yielded a monoexponential decay and was not further purified. The labeling reaction was carried out as follows: 1.0 g OIB−MA was dissolved in 8 mL of dodecane. The solution was heated at 180 °C for 14 h under nitrogen atmosphere to convert the succinic acid in the polymer to its anhydride form. The conversion was monitored by FTIR. The solution was cooled to room temperature, and PMA (185 mg) was added. The reaction mixture was heated again at 180 °C for another 14 h. Part of the dodecane was distilled off under vacuum and the concentrated polymer solution was poured into acetone to isolate the labeled polymer. The labeled polymer was then dissolved in hexane and precipitated by acetone four to five times to remove all the unreacted PMA and later dried under vacuum.

Labeling of OIB−MA with PHZ. A 0.5 g sample of OIB−MA was dissolved in 30 mL of xylene, and 1 g of molecular sieves was added to the solution. The solution was heated under reflux for 14 h with an azeotropic setup under nitrogen atmosphere. The acid to anhydride conversion was monitored by IR spectroscopy (cf. Figure 1). The amount of xylene in the reaction mixture was reduced to 10 mL by distilling off the

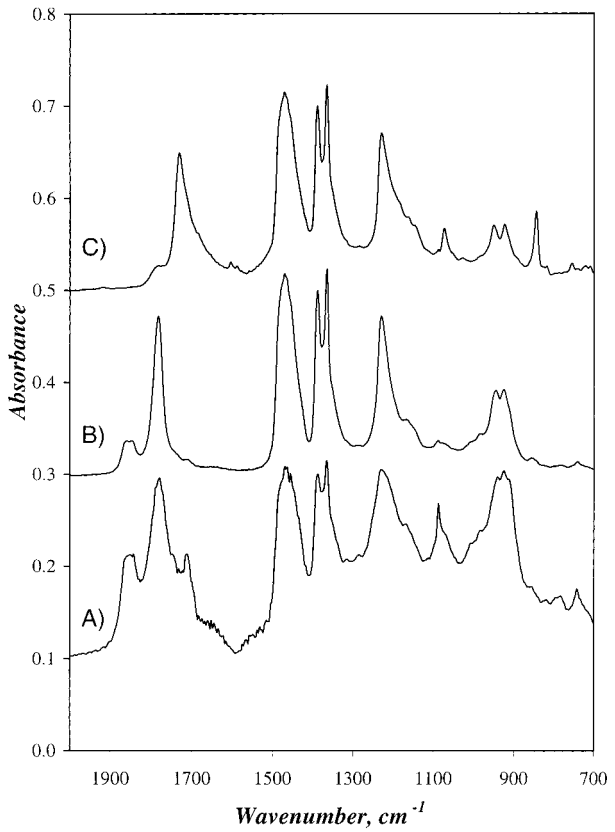

Figure 1. FTIR absorbance spectra of (A) Imperial Oil supplied OIB−MA after three precipitations from hexane into acetone, (B) the purified OIB−MA after having been kept overnight at 145 °C in refluxing xylene or 180 °C in dodecane, and (C) PHZ-labeled oligomer.

excess xylene. The solution was cooled to room temperature, and 136 mg of PHZ was added. The reaction mixture was heated again under reflux for another 18 h. The concentrated polymer solution was poured into acetone to isolate the labeled polymer. The labeled polymer was dissolved in hexane and centrifuged to remove any insoluble PHZ dye. The polymer was further purified by repeated dissolution into hexane and precipitation from acetone.

At low polymer concentration, the fluorescence exhibited by OIB−PHZ was very similar to that of OIB−PMA in either hexane or THF. Although PHZ was used as received for this labeling reaction, 1-pyrenebutanoic acid, which is its most likely fluorescent impurity, was certainly unable to react with OIB−MA and did not seem to affect the fluorescence behavior of OIB−PHZ.

Methylation of OIB−MA. The OIB−MA was methylated as reported elsewhere.[16] First, 0.66 g of OIB−MA was dissolved in 60 mL of toluene. Then, 200 μL of water was added, and the solution was heated under reflux for 1 h to hydrolyze all the anhydride functions. Following this, 2 g of molecular sieves was added to remove any unreacted water, and 6 mL of methanol was added to the solution. No precipitation occurred. The mixture was heated under reflux for 1 h. After the mixture was cooled to room temperature, trimethylsilyl diazomethane (400 μL of 2.0 M hexane solution) was added. The reaction mixture was stirred overnight under nitrogen at room temperature. Excess toluene was removed under vacuum, and the polymer was precipitated from toluene by acetone.

Methylation of OIB−PHZ. The reaction was carried out in the same manner as for the methylation of OIB−MA. Here, 0.1 g of OIB−PHZ was methylated, and the amounts of reactants used were scaled according to the procedure given in the above section.

Fourier Transform Infrared (FTIR) Spectroscopy. FTIR spectra were recorded on a MB-series Bomem spectrophotometer. The presence of MA attached onto the polymer could be detected by FTIR by monitoring the absorption peak at 1785 cm^{-1} characteristic of the carbonyl groups. After OIB−MA had reacted with PMA or PHZ, the peak at 1785 cm^{-1} disappeared and a new peak appeared at 1717 cm^{-1} characteristic of the presence of amide groups. In the case of OIB−MA, the MA content of the oligomer could be obtained from the ratio of the absorption at 1785 cm^{-1} (abs(1785 cm^{-1})) over the absorption at 1390 cm^{-1} (abs(1390 cm^{-1})) characteristic of the naked oligoisobutylene according to eq 1,[17] where N_{MA}

$$\frac{N_{MA}}{N_{IB}} = 0.024 \times \frac{\text{abs}(1785\ \text{cm}^{-1})}{\text{abs}(1390\ \text{cm}^{-1})} \quad (1)$$

and N_{IB} represent the number of MA and isobutylene units, respectively.

Absorption Measurements. Absorption spectra were recorded on a Hewlett-Packard 8452A diode array spectrophotometer. The pyrene contents of both labeled polymers were determined as reported elsewhere[9] and found to equal 3.3×10^{-4} and 2.6×10^{-4} mol/g for OIB−PMA and OIB−PHZ, respectively.

Steady-State Fluorescence Measurements. Fluorescence spectra were recorded on a Photon Technology International LS-100 steady-state system with a pulsed xenon flash lamp as the light source. Spectra of polymer solutions having a concentration above 1 g/L were obtained using the front face geometry. The spectra of more dilute solutions were obtained with the usual right angle configuration. The solutions were degassed under a gentle flow of nitrogen. The samples were excited at 344 nm and the fluorescence intensities of the monomer (I_M) and of the excimer (I_E) were obtained by taking the integrals under the fluorescence spectra from 372 to 378 nm for the monomer and from 500 to 530 nm for the excimer.

Time-Resolved Fluorescence Measurements. Fluorescence decay curves were obtained by the time-correlated single photon counting technique with a Photochemical Research Associates Inc. System 2000. The excitation wavelength was set at 344 nm, and the fluorescence from the pyrene monomer and excimer were monitored at 375 and 510 nm, respectively. To block potential light scattering leaking through the detection system, filters were used with a cutoff at 370 and 495 nm for the pyrene monomer and excimer, respectively. All decays were collected over 512 channels. A total of 20 000 counts were collected at the peak maximum of the lamp and the decay curves. The polymer solutions were degassed under a gentle flow of nitrogen. At polymer concentrations lower than 1 g/L, fluorescence decays were collected with a right angle configuration. At higher polymer concentrations, the front face geometry was used. The analysis of the decay curves were performed with the δ-pulse deconvolution.[18] Reference decay curves of degassed solutions of PPO [2,5-diphenyloxazole] in cyclohexane (τ = 1.42 ns)[19a] and BBOT [2,5-bis(5-*tert*-butyl-2-benzoxazolyl)thiophene] in ethanol (τ = 1.47 ns)[19b] were used for the analysis of the monomer and excimer decay curves, respectively.

Analysis of the OIB−Py Fluorescence Decays. First the fluorescence decays of the monomer and excimer were fitted with two or three exponentials according to eq 2, where n_{exp}

$$i_X(t) = \sum_{k=1}^{n_{exp}} a_{Xk} \exp(-t/\tau_{Xk}) \quad (2)$$

equals 2 or 3 and X equals M or E, whether one considers the fluorescence decay of the monomer or the excimer, respectively. Only for OIB−PHZ in hexane was n_{exp} equal to 3. Since the parameters retrieved from Scheme 1 for both OIB−Pys did not satisfy all conditions required by the Birks' model, Scheme 3 and Scheme 4 were introduced to describe the process of excimer formation between OIB−Py molecules.

Scheme 3. Analysis of the fluorescence decays according to Scheme 3 led to a set of four differential equations, which have been solved in Appendix A. According to this derivation, the fluorescence decays of the pyrene monomer ($i_M(t)$) and

Scheme 3. Modified Birks' Scheme, Which Accounts for the Presence of Ground-State Pyrene Dimers

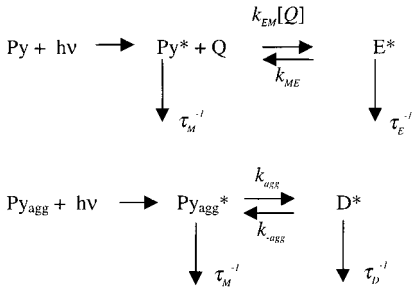

Scheme 4. Sequential Model

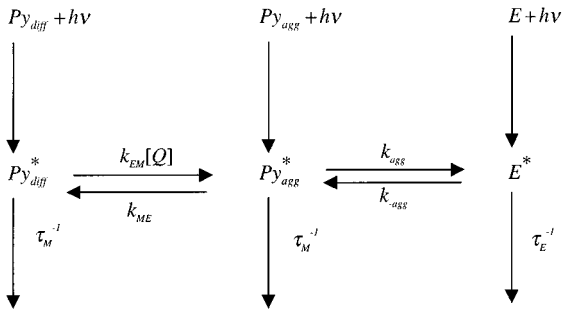

excimer ($i_E(t)$) are expected to be fitted by three and four exponentials, respectively. Their expressions are given in eqs 3 and 4 for the monomer and excimer, respectively.

$$i_M(t) = a_{M1}\exp(-t/\tau_1) + a_{M2}\exp(-t/\tau_2) + a_{M3}\exp(-t/\tau_3) \quad (3)$$

$$i_E(t) = a_{E1}\exp(-t/\tau_1) + a_{E2}\exp(-t/\tau_2) + a_{E3}\exp(-t/\tau_3) + a_{E4}\exp(-t/\tau_D) \quad (4)$$

In eqs 3 and 4, the two first exponentials are equivalent to those obtained with Birks' scheme.[6] Consequently, the decay times τ_1 and τ_2 are the same in the monomer and excimer decays, and the ratio a_{E1}/a_{E2} is expected to equal −1.0.

$i_M(t)$ and $i_E(t)$ were convoluted with the instrument response function $L(t)$ to yield $I_M(t)$ and $I_E(t)$, respectively. The light scattering correction was implemented by adding the instrument response function to the convolution product according to eq 5, where the symbol ⊗ indicates the convolution and a_{scattX}

$$I_X(t) = i_X(t) \otimes L(t) + a_{scattX}\,L(t) \quad (5)$$

represents the fraction of light scattering correction being applied to the monomer (X = M) and excimer (X = E) decays. Because of the difficulties associated with the analysis of fluorescence decays involving several decay times, the monomer and excimer decays were fitted simultaneously. In the analysis, the decay times τ_1, τ_2, and τ_3 were forced to remain the same for the monomer and the excimer decays, and the ratio a_{E1}/a_{E2} was kept equal to −1.0. The lifetime of D* in Scheme 3 (τ_D) could not be determined directly and it needed to be fixed in the analysis. Several values were tried ranging from 40 up to 70 ns, which correspond to a typical range of values for the pyrene excimer lifetime.[6] The kinetic parameters retrieved from the analysis were not much affected by the different τ_D values. However since the excimer lifetime τ_E was found to be close to 50 ns, all fluorescence decays were fitted with a τ_D value of 50 ns. This procedure allowed us to reduce the number of independent parameters.

Scheme 4. The fitting parameters retrieved from the fluorescence decay analysis for OIB−PHZ in hexane did not satisfy all conditions required by Birks' model and Scheme 3. Consequently Scheme 4 was introduced to describe the process of excimer formation between OIB−PHZ molecules in hexane.

Analysis of the OIB−PHZ fluorescence decays according to Scheme 4 led to a set of three differential equations, which have been solved in Appendix B. According to this derivation, the fluorescence decays of the pyrene monomer ($i_M(t)$) and excimer ($i_E(t)$) are expected to be fitted by three exponentials.

$$i_M(t) = a_{M1}\exp(-t/\tau_1) + a_{M2}\exp(-t/\tau_2) + a_{M3}\exp(-t/\tau_3) \quad (6)$$

$$i_E(t) = a_{E1}\exp(-t/\tau_1) + a_{E2}\exp(-t/\tau_2) + a_{E3}\exp(-t/\tau_3) \quad (7)$$

$i_M(t)$ and $i_E(t)$ were convoluted with the instrument response function $L(t)$ according to eq 5 to yield $I_M(t)$ and $I_E(t)$, respectively. As for the analysis of the fluorescence decays according to Scheme 3, the monomer and excimer decays were fitted simultaneously and the decaytimes τ_1, τ_2, and τ_3 were forced to remain the same for the monomer and the excimer decays.

The resulting functions $I_M(t)$ and $I_E(t)$ were used to fit simultaneously the experimental monomer and excimer fluorescence decays, and the parameters were optimized using the Marquardt−Levenberg algorithm.[20] The goodness of the fit was estimated by the χ^2 parameter (a good fit yields a $\chi^2 < 1.30$) and the random distribution of the residuals and of the autocorrelation function of the residuals around zero.

Viscosity Measurements. The viscosity of the OIB−MA solutions in THF were measured with an Ubbelohde viscometer. The viscosity of the polymer solution was found to depend on the polymer concentration according to eq 8, where the

$$\eta = 0.44 + 0.0033[\text{Poly}] \quad (8)$$

viscosity η and the polymer concentration are expressed in mPa·s and g/L, respectively.

Field Desorption Mass Spectrometry (FD MS): FD MS experiments were done with a ZabSpec-oa-TOF Ultima double-focusing mass spectrometer (Micromass, Manchester, U.K.). The instrument was tuned for 2000 resolving power. The accelerating voltage was 4000 V. The mass range 400−4000 Da was scanned at 5 s/mass decade. Data were acquired in the continuum mode. 1 μL of sample (∼5% in methylene chloride) was deposited onto the FD emitter. The emitter current was increased manually from 0 to 90 mA during the run. The majority of the signal was collected in the emitter current range 35−45 mA. The mass spectrum reported was obtained by averaging the accumulated mass spectra over the entire run.

Error Determination. For each set of preexponential factors and decaytimes retrieved from the analysis of the experimental fluorescence decays, 20 fluorescence decays for the monomer and the excimer were simulated with 20 different Poisson noise patterns.[21] The same analysis was repeated with the 20 simulated decays and the averages and standard deviations of the retrieved preexponential factors and decaytimes were calculated. Each one of the 20 sets of preexponential factors and decaytimes was used to calculate 20 different sets of kinetic parameters used in Schemes 3 and 4. These 20 sets of kinetic parameters allowed us to calculate the standard deviations, which are reported for all the parameters listed in Tables 2−6 and provide an estimate of the spread of the errors.

Results

In this report, we set out to characterize the microstructure and associative strength of OIB−MA by monitoring the fluorescence of a dye attached onto the succinic anhydride moieties. To obtain a satisfying correspondence between the dye's response and the OIB−MA microstructure and associative strength, it was important to establish that most succinic anhydride moieties were labeled. This in turn required a thorough characterization of the OIB−MA sample, such as its molecular weight and level of grafting. These parameters were characterized by a combination of several

Table 1. Estimated Molecular Weights and MA Grafting Levels (Given in Parentheses as 1 MA Unit per *x* Isobutylene Units [1/*x*]) of the Naked OIB−MA, the Methylated OIB−MA, and the OIB−Pys

sample name	OIB−MA	OIB−PMA	OIB−PHZ
FTIR[a]	2700 [1/48]		
^{1}H NMR[b]	3000 [1/53]		
UV/vis abs[c]		2800 [1/50]	3500 [1/62]
mass spectrom		2200 ± 100 [1/38]	2500 ± 100 [1/38]

[a] An FTIR spectrum of the OIB−MA sample was obtained after the sample had been purified prior pyrene labeling. The ratio abs(1785 cm^{-1})/abs(1390 cm^{-1}) was measured and equaled 0.86. Using eq 1, it was found that there was one succinic anhydride unit per 48 isobutylene units. [b] OIB−MA was hydrolyzed and reacted with methanol in order to form the dimethyl ester, as reported by Liu et al.[16] The signal from the methyl groups could be easily detected at 3.6 ppm by ^{1}H NMR. An NMR-based estimate of M_n could be achieved by assuming that all succinic acid units are methylated. The area under the methyl ester peak was compared with the area under the peaks of the backbone protons located between 0.6 and 1.6 ppm. The ratio of both areas was calculated, and the number of isobutylene units per succinic anhydride moiety was calculated to be 53. [c] UV/vis absorption measurements in THF were applied to determine the M_n's of the pyrene-labeled OIB by using the extinction coefficient of a model compound, namely pyrenemethanol in THF (ϵ(pyrenemethanol at 344 nm) = 42 700 M^{-1}·cm^{-1}). These measurements showed that the OIB−Py contained one pyrene chromophore for 50 and 62 isobutylene units in OIB−PMA and OIB−PHZ, respectively.

techniques namely, FTIR, ^{1}H NMR, UV/vis absorption and mass spectrometry (MS). The results are shown in Table 1. FTIR and ^{1}H NMR measurements were carried out on the unlabeled OIB−MA and the methylated OIB−MA polymer, respectively. UV/vis absorption measurements were performed on the labeled polymer. All three techniques compare the number of MA units with respect to the number of isobutylene units in the OIB−MA sample.

Whereas the calculation of the molecular weights by FTIR, ^{1}H NMR, and UV/vis absorption listed in the first three rows of Table 1 is based on the assumption that each OIB chain contains a single MA unit, MS yields the absolute molecular weights of OIB−MA and the OIB−Pys. The MS spectra exhibited a low intensity, broad, noisy hump centered around 2200 ± 100 for OIB−MA and 2500 ± 100 for OIB−PMA and OIB−PHZ, meaning that the naked oligomer is made of 38 ± 2 isobutylene units. This value is much shorter than the value of 51 ± 3 isobutylene units obtained by FTIR, ^{1}H NMR, and UV/vis measurements carried out on OIB−PMA. The discrepancy between the two values is certainly due to the fact that some chains do not display any MA moiety.

FTIR, ^{1}H NMR, and UV/vis measurements carried out on OIB−PMA yield a molecular weight value of 2850 ± 150 or 51 ± 3 isobutylene units per MA moiety. The larger molecular weight obtained with OIB−PHZ by UV/vis absorption (cf. Table 1) indicates that less pyrene is attached onto the oligomer. Actually 18% of the MA moieties have not reacted. Differences in M_n values observed by UV/vis absorption can arise from differences in labeling efficiencies between PMA and PHZ, assuming that PHZ is being less reactive than PMA. To investigate this possibility, OIB−PHZ was methylated. UV/vis absorption measurements showed that the methylation reaction had not affected the pyrene content of the polymer. ^{1}H NMR spectra of the methylated OIB−PHZ sample exhibited a small and noisy peak at 3.6 ppm. Comparison of the area under the methyl ester peak at 3.6 ppm, and the area under the backbone protons indicated that 25% of the MA moieties had been methylated. This result agrees qualitatively with the UV/vis measurements carried out with OIB−PHZ, leading to the conclusion that, under our experimental conditions, PHZ does not react as well with OIB−MA as PMA does. Numerous PHZ labeling reactions were carried out in an attempt to improve the reaction yield. Toluene, xylene and dodecane are three high boiling point solvents, which were tried. For each one of these solvents, the PHZ labeling reaction was performed at different temperatures and over different lengths of time. The best labeling result was obtained by carrying the reaction in refluxing xylene, as reported in the Experimental section, yielding one pyrene moiety per 62 isobutylene units.

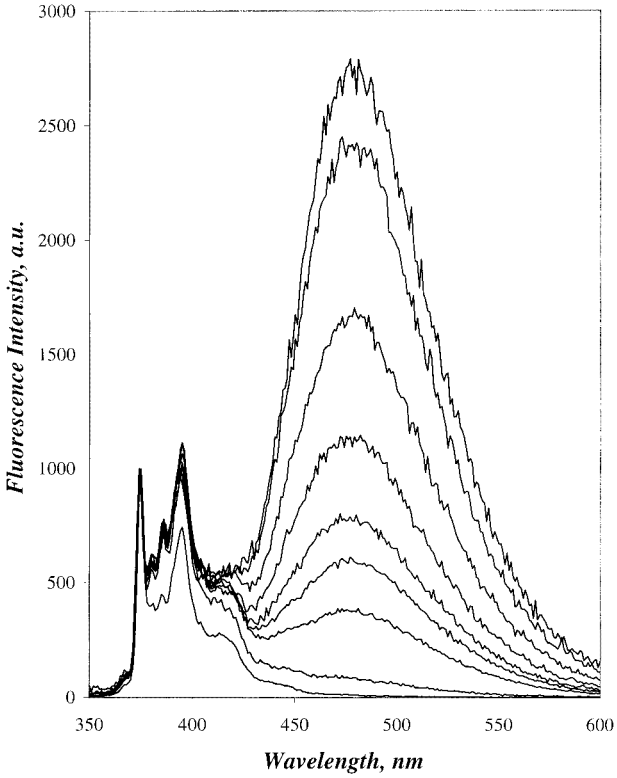

Figure 2. Steady-state fluorescence spectra of the PMA and OIB−PMA in THF with λ_{ex} = 344 nm. From bottom to top: the dye PMA at a concentration of 2.5 × 10^{-6} M, OIB−PMA at a concentration of 2.5 × 10^{-6} M or 0.008, 7.4, 17, 26, 45, 67, 119, or 163 g·L^{-1}.

Steady-state and time-resolved fluorescence experiments were carried out on both polymers in THF and hexane. The fluorescence intensities of the monomer (I_M) and of the excimer (I_E) were measured by taking the area under the fluorescence trace from 372 to 378 nm and from 500 to 530 nm, respectively. As shown in Figure 2 for OIB−PMA in THF, excimer formation increases with polymer concentration. However even at very low polymer concentration, a nonzero fluorescence emission is observed around 500 nm, which does not exist in the PMA fluorescence spectrum in THF. This behavior was observed for both dyes either in THF or hexane. This indicates that intramolecular excimer formation is taking place, and that some OIB−MA bear more than one MA unit per chain. The ratios I_E/I_M were plotted as a function of oligomer concentration in Figure 3. Despite the spectral differences observed in the vibronic structure of the pyrene monomers for OIB−

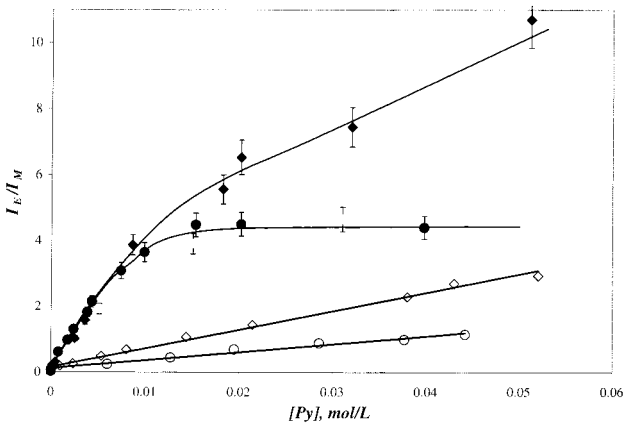

Figure 3. Plot of the I_E/I_M ratio vs pyrene concentration for OIB−PMA (pyrene content = 3.3×10^{-4} mol/g of oligomer) in THF (◇) and in hexane (◆) and for OIB−PHZ (pyrene content = 2.6×10^{-4} mol/g of oligomer) in THF (○) and in hexane (●, nonmethylated sample; gray circle, methylated sample).

PMA and OIB−PHZ in hexane and in THF, which prevent any direct comparison between the graphs, the overall shape of the I_E/I_M ratios vs OIB−Py concentration is still informative. In THF the I_E/I_M ratios increase linearly over the whole oligomer concentration range for both OIB−Pys, as predicted by the Birks' Scheme.[6] This is not so in hexane. Below a pyrene concentration of about 0.01 mol/L (equivalent to OIB−PMA and OIB−PHZ concentrations of 30 and 40 g/L, respectively), the ratio I_E/I_M increases linearly with oligomer concentration in hexane. Above the pyrene concentration of 0.01 mol/L, the ratio I_E/I_M plateaus for OIB−PHZ, and increases more slowly for OIB−PMA. This behavior is very different from the one observed in THF.

Polyolefins grafted with MA and labeled with PMA or PHZ are known to aggregate in apolar solvents via their polar moieties,[12,13] and the trends displayed in Figure 3 can be explained on the basis of associations occurring between OIB−Pys. Traditionally an increase in pyrene concentration yields more diffusional encounters between pyrenes and the ratio I_E/I_M increases. This is indeed well predicted by the classic Birks' scheme for which the ratio I_E/I_M is directly proportional to the pyrene concentration[6] and is observed for both OIB−Pys in polar THF where no associations are expected to occur. However if OIB−Pys form aggregates in hexane via their polar moieties and the solution is made up of pyrene aggregates, excimer formation occurs only inside a pyrene aggregate. Addition of more pyrene groups results in the formation of more OIB−Py aggregates, which produce excimer in the same manner. The process of excimer formation is switched from an intermolecular diffusion-controlled process between separated pyrene groups to an intramolecular process between pyrene groups located inside the pyrene aggregates. Consequently, the ratio I_E/I_M becomes independent of pyrene concentration as observed in Figure 3 for OIB−PHZ solutions in hexane at concentrations larger than 40 g/L. The trend observed in Figure 3 for OIB−PMA in hexane could be an intermediate case between the two extreme cases, namely OIB−Pys in THF where no intermolecular associations are taking place, and OIB−PHZ in hexane where all chains are associated for oligomer concentrations above 40 g/L.

To investigate these hypotheses, fluorescence decay measurements were carried out. Typical traces for oligomer concentrations of about 120 g/L are shown for

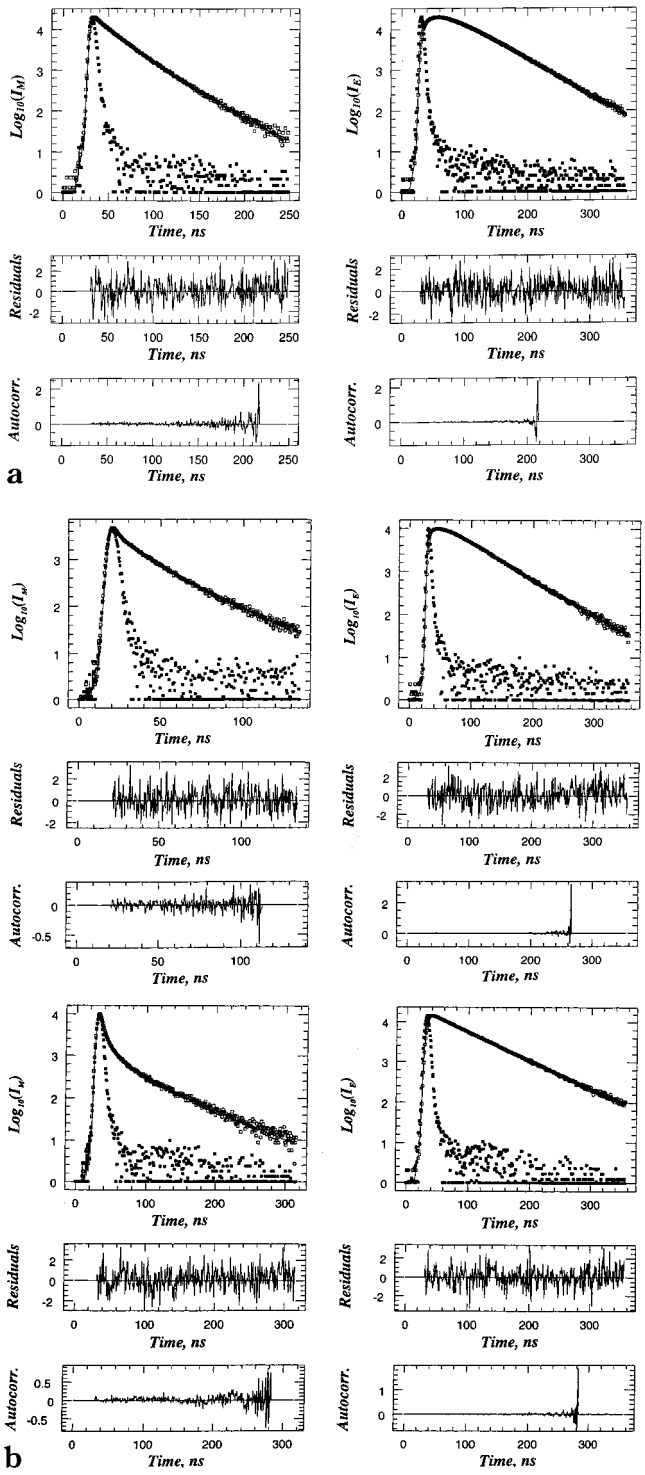

Figure 4. Fluorescence decays of the monomer (left) and the excimer (right) for (a) OIB−PMA in THF at 119 g/L and (b) OIB−PMA in hexane at 120 g/L (top panel) and OIB−PHZ in hexane at 117 g/L (bottom panel). The samples were excited at 344 nm and the fluorescence emission of the monomer and excimer were collected at 375 and 510 nm, respectively.

the pyrene monomer and excimer for OIB−PMA in THF in Figure 4a, for OIB−PMA in hexane in Figure 4b (top), and for OIB−PHZ in hexane in Figure 4b (bottom). In THF, both OIB−PMA and OIB−PHZ had exactly the same behavior and only one set of data is represented in Figure 4a. However differences between the decays obtained in hexane are striking. Whereas the monomer and excimer decays of OIB−PMA in hexane are very similar to those obtained for both OIB−Pys in THF, the

monomer and excimer decays of OIB−PHZ exhibit a clearly distinct behavior. The fluorescence decay of the OIB−PHZ monomer presents a pronounced fluorescence reduction at the early times. The rise time of the excimer, which is clearly visible for OIB−PMA in hexane and for both OIB−Pys in THF, can hardly be detected by a naive ocular inspection of the excimer decay of OIB−PHZ in hexane.

To account for these effects in a more quantitative manner, the fluorescence decays of both OIB−Pys in THF and of OIB−PMA in hexane were fitted with a sum of two exponentials, but three exponentials were required to fit the fluorescence decays of OIB−PHZ in hexane. The decay times and preexponential factors retrieved from the fits are listed in Table 2 parts A−D). At very low oligomer concentration, the fluorescence decays of the pyrene monomer were biexponential in all solvents. This behavior is attributed to the presence of oligoMA attached onto some of the OIB chains, which induces intramolecular excimer formation, as was observed by steady-state fluorescence. The long decay time obtained with more than 80% of the total preexponential weight was attributed to the lifetime τ_M of pyrenes attached onto single MA units. Thus, τ_M was found to equal 290 and 210 ns for OIB−PMA and OIB−PHZ in THF, respectively, and 356 and 263 ns for OIB−PMA and OIB−PHZ in hexane, respectively.

Although the pyrene monomer and excimer decays of both OIB−Pys in THF and OIB−PMA in hexane could be fitted with two exponentials as requested by Birks' scheme, several other conditions requested by Birks' scheme were not fulfilled. For instance the decay times of the monomer never matched those of the excimer and the ratios of the preexponential factors of the excimer decays never equaled −1.00. The OIB−PHZ decays in hexane did not follow Birks' scheme either since three exponentials were required to fit the decays. The decays of OIB−PHZ in hexane had also well-defined features. A short decay time (τ_{M1}) of 8.9 ± 1.8 ns is obtained for the OIB−PHZ monomer decays, which is paralleled by a short rise time (τ_{E1}) of 9.2 ± 3.3 ns for the OIB−PHZ excimer decay. This short decay/rise time indicates that pyrenes are forming excimer on a fast time scale, or in other terms that some pyrenes are close to one another, as they would be inside pyrene aggregates. For all excimer decays of OIB−PHZ in hexane, the decay time τ_{E2} equals 57 ± 7 ns and is obtained with the strongest contribution. This τ_{E2} value is also typical for the pyrene excimer lifetime.[6]

The first exponential in the fluorescence decays of the OIB−PHZ monomer and excimer in hexane always exhibits a short decay time. If its contribution is attributed to that arising from excited pyrenes located inside pyrene aggregates, the normalized preexponential factor a_{M1} can be taken as a representation of the fraction of pyrene groups, which are located inside pyrene aggregates. A plot of a_{M1} vs OIB−PHZ concentration is given in Figure 5. Below a pyrene concentration of 0.0005 M (equivalent to an oligomer concentration of 1.9 g/L), a_{M1} equals zero. Above this concentration, a_{M1} increases with oligomer concentration until it reaches a plateau for pyrene concentrations larger than 0.01 M (equivalent to an oligomer concentration of 40 g/L). The presence of a plateau would indicate that the fraction of pyrenes located inside pyrene aggregates does not change above 40 g/L, which would follow from a complete aggregation of the OIB−PHZ molecules. Interestingly this explanation agrees with that proposed earlier in order to explain the behavior of the ratio I_E/I_M of OIB−PHZ in hexane, which was also found to plateau for pyrene concentrations larger than 0.01 M (cf. Figure 3).

Another parameter, which gives information about the nature of the pyrene excimer, is the ratio $(a_{E1}/(a_{E2} + a_{E3}))$, where a_{E1} is the rise time contribution of the excimer decay and has a negative amplitude and a_{E2} and a_{E3} are the positive amplitudes of the excimer decay. For OIB−PMA in hexane and OIB−PMA and OIB−PHZ in THF, a_{E3} equals zero. If no preassociated pyrenes are present and excimers are formed via a purely diffusional process, the ratio $(a_{E1}/(a_{E2} + a_{E3}))$ must equal −1.00. If this ratio is more positive than −1.00, pyrene ground-state dimers are present. The more positive the ratio and the more pyrene ground-state dimers are present. Thus, the ratio $(a_{E1}/(a_{E2} + a_{E3}))$ gives information about the nature of the excimer, which is being formed, and it was plotted against oligomer concentration in Figure 6. Within experimental error, the ratio remains constant with oligomer concentration for a given oligomer and solvent. It was found to equal −0.87 ± 0.01 for OIB−PMA and OIB−PHZ in THF, −0.68 ± 0.07 for OIB−PMA in hexane, and −0.23 ± 0.09 for OIB−PHZ in hexane. The following conclusions can be drawn from these results: (1) Pyrene excimers are formed mostly via intermolecular diffusional encounters in THF, where the ratio $(a_{E1}/(a_{E2} + a_{E3}))$ is close to −1.00 for both OIB−PMA and OIB−PHZ. (2) Pyrene excimers are formed mostly from the excitation of pyrene ground-state dimers for OIB−PHZ in hexane, where the ratio $(a_{E1}/(a_{E2} + a_{E3}))$ is the most positive and equals −0.23 ± 0.09. (3) Pyrene excimers are formed via both diffusional encounters and excitation of pyrene ground-state dimers for OIB−PMA in hexane, where the ratio $(a_{E1}/(a_{E2} + a_{E3}))$ takes an intermediate value and equals −0.68 ± 0.07.

It might be surprising at first sight that the ratio $(a_{E1}/(a_{E2} + a_{E3}))$ for OIB−PHZ in hexane remains constant as the oligomer concentration decreases whereas the preexponential factor a_{M1} undergoes a substantial drop. Both parameters are claimed to represent the pyrene aggregate population and would be expected a priori to behave in a similar manner. However this last statement is not true. The ratio $(a_{E1}/(a_{E2} + a_{E3}))$ yields qualitative information about the fraction of *all* pyrenes present as ground-state dimers. The preexponential factor a_{M1} is related to the fraction of *only* pyrene monomers involved in pyrene aggregates. At very low polymer concentration where no intermolecular association takes place, no pyrene aggregate is formed and the fraction of pyrene monomers involved into pyrene aggregates is nil and a_{M1} equals zero, as observed in Figure 5. However even at these low polymer concentrations, pyrene ground-state dimers are present due to the presence of oligoMA and the ratio $(a_{E1}/(a_{E2} + a_{E3}))$ does not equal zero. Thus, although both parameters report similar information about the process of excimer formation, they are not expected to behave in a similar manner.

The features of the fluorescence decays exhibited by the OIB−PHZ excimer in hexane are typical of those of an excimer formed inside a pyrene aggregate. Typically the fluorescence decay of the pyrene excimer formed in a system, which yields pyrene aggregates, will exhibit

Table 2. Parameters Obtained from the Biexponential Fit of Fluorescence Decays of OIB−PMA and OIB−PHZ in THF and Hexane[a]

A. OIB−PMA in THF

[OIB] (g/L)	τ_{M1} (ns)	a_{M1}	τ_{M2} (ns)	a_{M2}	χ^2	τ_{E1} (ns)	a_{E2}	τ_{E1} (ns)	a_{E2}	χ^2
0.007	84 ± 4	0.21 ± 0.01	290 ± 1	0.79 ± 0.01	1.10	n.a.	n.a.	n.a.	n.a.	n.a.
26	28 ± 2	0.18 ± 0.01	92 ± 0	0.82 ± 0.01	1.14	39 ± 0	−0.71 ± 0.00	89 ± 0	1.00	1.14
45	17 ± 1	0.22 ± 0.01	62 ± 0	0.78 ± 0.01	1.14	37 ± 0	−0.84 ± 0.00	69 ± 0	1.00	1.17
67	29 ± 1	0.38 ± 0.04	51 ± 1	0.62 ± 0.04	1.29	34 ± 0	−0.87 ± 0.00	58 ± 0	1.00	1.13
119	18 ± 0	0.50 ± 0.03	32 ± 0	0.50 ± 0.03	1.29	21 ± 0	−0.86 ± 0.00	48 ± 0	1.00	1.04
134	15 ± 1	0.38 ± 0.02	29 ± 0	0.62 ± 0.02	1.09	23 ± 0	−0.86 ± 0.00	47 ± 0	1.00	1.33
163	22 ± 0	0.90 ± 0.02	40 ± 1	0.10 ± 0.02	1.13	20 ± 0	−0.86 ± 0.00	45 ± 0	1.00	1.03

B. OIB−PHZ in THF

[OIB] (g/L)	τ_{M1} (ns)	a_{M1}	τ_{M2} (ns)	a_{M2}	χ^2	τ_{E1} (ns)	a_{E2}	τ_{E1} (ns)	a_{E2}	χ^2
0.009	105 ± 9	0.17 ± 0.03	210 ± 2	0.83 ± 0.03	1.25	n.a.	n.a.	n.a.	n.a.	n.a.
49	33 ± 1	0.26 ± 0.01	70 ± 0	0.74 ± 0.01	1.26	39 ± 0	−0.86 ± 0.00	72 ± 0	1.00	1.14
75	24 ± 1	0.29 ± 0.02	52 ± 0	0.72 ± 0.02	1.13	35 ± 0	−0.89 ± 0.00	58 ± 0	1.00	1.14
110	23 ± 0	0.55 ± 0.02	42 ± 0	0.46 ± 0.02	1.34	27 ± 0	−0.88 ± 0.00	52 ± 0	1.00	0.98
145	17 ± 1	0.35 ± 0.02	36 ± 0	0.65 ± 0.02	1.19	26 ± 0	−0.87 ± 0.00	51 ± 0	1.00	1.06

C. OIB−PMA in Hexane

[OIB] (g/L)	τ_{M1} (ns)	a_{M1}	τ_{M2} (ns)	a_{M2}	χ^2	τ_{E1} (ns)	a_{E2}	τ_{E1} (ns)	a_{E2}	χ^2
0.007	109 ± 5	0.17 ± 0.00	356 ± 1	0.83 ± 0.00	1.17	n.a.	n.a.	n.a.	n.a.	n.a.
8	31 ± 1	0.19 ± 0.00	115 ± 0	0.81 ± 0.00	1.30	44 ± 1	−0.62 ± 0.00	113 ± 0	1.00	1.19
12	29 ± 1	0.21 ± 0.01	91 ± 0	0.79 ± 0.01	1.18	44 ± 0	−0.73 ± 0.00	91 ± 0	1.00	1.22
27	19 ± 1	0.26 ± 0.01	48 ± 0	0.74 ± 0.01	1.24	n.a.	n.a.	n.a.	n.a.	n.a.
53	11 ± 0	0.25 ± 0.01	31 ± 1	0.75 ± 0.01	1.08	25 ± 0	−0.76 ± 0.00	54 ± 0	1.00	1.46
63	18 ± 0	0.59 ± 0.02	33 ± 0	0.41 ± 0.02	1.14	23 ± 0	−0.75 ± 0.00	54 ± 0	1.00	0.98
100	16 ± 0	0.62 ± 0.02	31 ± 0	0.38 ± 0.02	1.08	20 ± 0	−0.71 ± 0.00	53 ± 0	1.00	1.10
120	14 ± 0	0.65 ± 0.01	28 ± 0	0.35 ± 0.01	1.22	17 ± 0	−0.62 ± 0.00	48 ± 0	1.00	1.18
160	12 ± 0	0.81 ± 0.01	26 ± 0	0.19 ± 0.01	1.03	13 ± 0	−0.62 ± 0.00	51 ± 0	1.00	1.10

D. OIB−PHZ in Hexane

[OIB] (g/L)	τ_{M1} (ns) a_{M1}	τ_{M2} (ns) a_{M2}	τ_{M3} (ns) a_{M3}	χ^2	τ_{E1} (ns) a_{E1}	τ_{E2} (ns) a_{E2}	τ_{E3} (ns) a_{E3}	χ^2
0.009		82 (±12)	263 (±1)	1.15	n.a.	n.a.	n.a.	n.a.
		0.07 (±0.01)	0.93 (±0.01)					
0.1		20.4 (±1)	218 (±0)	1.18	8.0	61 (±0)	189 (±3)	1.04
		0.13 (±0.01)	0.87 (±0.01)		0.01	1.00	0.09 (±0.01)	
0.4	8.5 (±1.0)	64 (±10)	229 (±1)	1.11	n.a.	n.a.	n.a.	n.a.
	0.23 (±0.01)	0.08 (±0.01)	0.69 (±0.01)					
0.6	11.3 (±0.7)	170 (±10)	241 (±20)	0.99	8.6 (±0.8)	61 (±0)	198 (±3)	1.11
	0.22 (±0.01)	0.55 (±0.12)	0.24 (±0.12)		−0.15 (±0.01)	1.00	0.11 (±0.00)	
3.0	13.1 (±0.5)	122 (±8)	175 (±10)	1.07	8.1 (±0.6)	56 (±1)	125 (±2)	1.11
	0.35 (±0.01)	0.47 (±0.10)	0.18 (±0.10)		−0.24 (±0.01)	1.00	0.15 (±0.01)	
6.8	10.1 (±0.3)	92 (±7)	156 (±2)	1.12	9.7 (±0.7)	56 ± (1)	122 (±2)	0.99
	0.50 (±0.01)	0.19 (±0.02)	0.31 (±0.02)		−0.22 (±0.01)	1.00	0.18 (±0.02)	
9.3	7.4 (±0.3)	39 (±3)	135 (±1)	1.03	8.1 (±0.6)	56 (±1)	115 (±2)	1.11
	0.52 (±0.01)	0.14 (±0.01)	0.34 (±0.00)		−0.24 (±0.01)	1.00	0.19 (±0.02)	
15	8.4 (±0.2)	44 (±4)	124 (±1)	1.01	9.6 (±1.0)	52 (±2)	92 (±2)	1.09
	0.58 (±0.01)	0.13 (±0.00)	0.29 (±0.01)		−0.25 (±0.02)	1.00	0.42 (±0.08)	
20[b]	8.4 (±0.3)	34 (±3)	96 (±1)	1.36	8.7 (±0.8)	52 (±2)	85 (±2)	1.03
	0.58 (±0.01)	0.14 (±0.01)	0.28 (±0.00)		−0.29 (±0.03)	1.00	0.36 (±0.12)	
24	8.7 (±0.2)	52 (±4)	103 (±1)	1.04	7.8 (±1.2)	45 (±3)	75 (±1)	1.07
	0.62 (±0.01)	0.16 (±0.01)	0.21 (±0.01)		−0.21 (±0.02)	0.55 (±0.07)	0.66 (±0.08)	
28	9.6 (±0.3)	27 (±3)	55 (±1)	1.39	10.4 (±3.1)	55 (±3)	38 (±6)	1.18
	0.58 (±0.03)	0.19 (±0.02)	0.22 (±0.02)		−0.27 (±0.19)	1.00	0.92 (±0.65)	
38	7.4 (±0.2)	26 (±2)	81 (±1)	1.10	18.7 (±1.2)	70 (±0)	28 (±1)	0.97
	0.63 (±0.01)	0.13 (±0.01)	0.24 (±0.01)		−0.49 (±0.19)	1.00	0.66 (±0.19)	
58[b]	6.0 (±0.1)	21 (±1)	65 (±1)	1.06	8.0 (±0.6)	65 (±2)	42 (±5)	1.10
	0.66 (±0.01)	0.17 (±0.01)	0.17 (±0.00)		−0.23 (±0.03)	1.00	0.40 (±0.22)	
59	8.5 (±0.1)	35 (±2)	70 (±2)	1.35	11.3 (±1.8)	64 (±1)	34 (±5)	0.96
	0.72 (±0.01)	0.17 (±0.01)	0.11 (±0.01)		−0.19 (±0.07)	1.00	0.29 (±0.06)	
78	7.5 (±0.2)	29 (±2)	56 (±1)	0.96	5.7 (±0.7)	62 (±0)		0.94
	0.60 (±0.01)	0.18 (±0.01)	0.22 (±0.02)		−0.16 (±0.01)	1.00		
117	6.5 (±0.3)	16 (±1)	57 (±0)	1.05	6.7 (±0.8)	51 (±3)	73 (±5)	1.01
	0.57 (±0.04)	0.29 (±0.04)	0.14 (±0.00)		−0.14 (±0.05)	1.00	0.42 (±0.40)	
153	7.2 (±1.5)	21 (±3)	48 (±1)	1.31	5.6 (±0.5)	55 (±1)	109 (±22)	1.04
	0.64 (±0.14)	0.23 (±0.12)	0.13 (±0.02)		−0.15 (±0.01)	1.00	0.03 (±0.03)	

[a] The samples were excited at λ_{ex} = 344 nm and the fluorescence emission was collected at λ_{em} = 375 nm and λ_{em} = 510 nm for the monomer and excimer, respectively. [b] Methylated OIB−PHZ sample.

either a short but little pronounced rise time (rise time <10 ns and $(a_{E1}/(a_{E2} + a_{E3})) < -0.3$) or no rise time.[10] In this laboratory, similar features were observed for a modified ethylene-propylene random copolymer labeled with PHZ in hexane[12] and various pyrene-labeled poly(ethylene oxide)s in water.[22]

In the case of a typical Stern−Volmer plot where a dye is quenched by a quencher Q, the following relation-

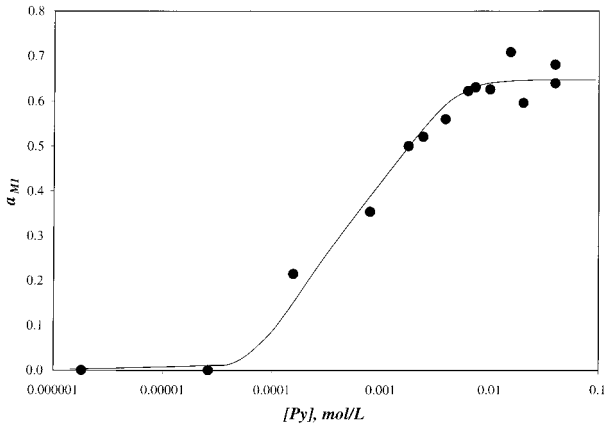

Figure 5. Plot of the normalized preexponential factor a_{M1} of the fluorescence decay of the OIB−PHZ monomer in hexane as a function of pyrene concentration (pyrene content = 2.6 × 10^{-4} mol/g of oligomer, ●, nonmethylated sample; gray circle, methylated sample).

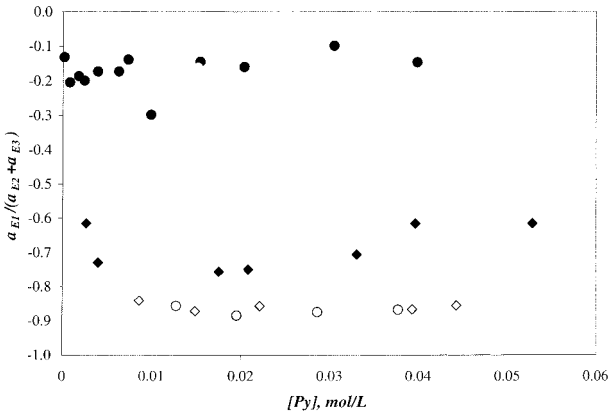

Figure 6. Ratio of the preexponential factors of the excimer decays as a function of pyrene concentration for OIB−PMA (pyrene content = 3.3 × 10^{-4} mol/g of oligomer) in THF (◇) and in hexane (◆) and for OIB−PHZ (pyrene content = 2.6 × 10^{-4} mol/g of oligomer) in THF (○) and in hexane (●; nonmethylated sample; gray circle, methylated sample).

ship is observed

$$\frac{I_0}{I} = 1 + k_Q\tau_M[Q] \tag{9}$$

where I is the fluorescence intensity of the dye at a given quencher concentration [Q], I_0 is the fluorescence intensity of the dye with no quencher, and τ_M is the dye's lifetime. In our experiments, the excited chromophore is an excited pyrene and the quencher is a ground-state pyrene. Although our fluorescence data do not behave ideally due to the presence of pyrene aggregates, the contribution of these aggregates to the monomer fluorescence decays must be limited to the early times, since excimer formation within an aggregate occurs on a fast time scale. Thus, as a first approximation, the integral under the monomer fluorescence decay, which is represented by $\langle\tau\rangle$ and is given in eq 10, can be taken as an estimate of the fluorescence intensity arising from diffusional phenomena so that $I \propto \langle\tau\rangle$.

$$\langle\tau\rangle = \frac{a_{M1}\tau_{M1} + a_{M2}\tau_{M2} + a_{M3}\tau_{M3}}{a_{M1} + a_{M2} + a_{M3}} \tag{10}$$

The parameters a_{Mi} and τ_{Mi} of eq 10 are listed in Table 2, parts A−D). Equation 9 can then be rewritten as eq 11 so that the difference in lifetimes for OIB−PMA and OIB−PHZ can be factored out.

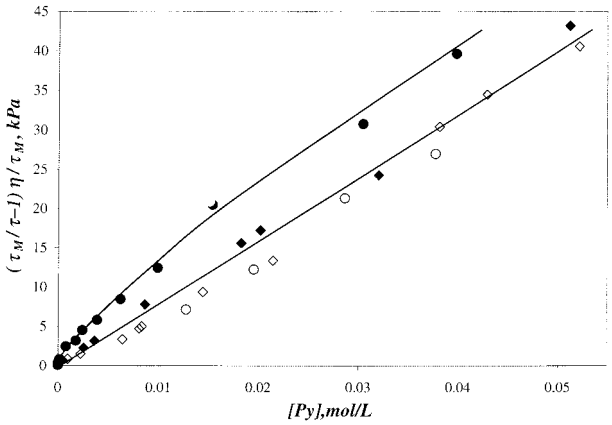

Figure 7. Plot of the quantity $((\tau_M/\langle\tau\rangle) - 1)(\eta/\tau_M)$ as a function of pyrene concentration for OIB−PMA (pyrene content = 3.3 × 10^{-4} mol/g of oligomer) in THF (◇) and in hexane (◆) and for OIB−PHZ (pyrene content = 2.6 × 10^{-4} mol/g of oligomer) in THF (○) and in hexane (●, nonmethylated sample; gray circle, methylated sample).

$$\left(\frac{\tau_M}{\langle\tau\rangle} - 1\right)\frac{1}{\tau_M} = k_Q[Q] \tag{11}$$

Because large amounts of oligomer are added to the solutions, the solution viscosity must be taken into account and the product $((\tau_M/\langle\tau\rangle) - 1)(\eta/\tau_M)$ is plotted as a function of pyrene concentration in Figure 7. As expected for a purely diffusion-controlled reaction, a linear relationship is obtained in Figure 7 for both OIB−Pys in THF and OIB−PMA in hexane and the product $\eta \times k_Q$ is given by the slope of the straight line and equals 780 ± 50 kPa·L·mol^{-1}. This analysis supports the claim that diffusional quenching is occurring for both OIB−Pys in THF and OIB−PMA in hexane.

The ratio $((\tau_M/\langle\tau\rangle) - 1)(\eta/\tau_M)$ behaves differently for OIB−PHZ in hexane. In this case, the quenchers, which an unassociated excited pyrene can encounter by diffusion, are ground-state pyrenes, which are either attached onto single MA units or onto oligoMA or are involved in pyrene aggregates. However if most pyrenes are involved into pyrene aggregates, excimer formation will occur inside a pyrene aggregate and will not be diffusion-controlled. Whereas the ratio $((\tau_M/\langle\tau\rangle) - 1)(\eta/\tau_M)$ yields a linear trend for OIB−PMA in hexane similar to that of both OIB−Pys in THF, a bent profile is observed for OIB−PHZ in hexane. Furthermore, at any given pyrene concentration in Figure 7, the quantity $((\tau_M/\langle\tau\rangle) - 1)(\eta/\tau_M)$ for OIB−PHZ in hexane lies above that for both OIB−Pys in THF and OIB−PMA in hexane. This behavior indicates that the quenching of an excited pyrene monomer is more efficient for OIB−PHZ in hexane than the three other oligomer/solvent combinations considered. This enhanced quenching is certainly the result of pyrene associations. In hexane, most OIB−PHZ molecules are involved into aggregates and an excited pyrene monomer forms excimer readily inside the pyrene aggregate on a much faster time scale than by diffusion. Diffusional quenching occurs when fewer or no aggregates are present such as for OIB−PMA in hexane and both OIB−Pys in THF.

The data obtained for OIB−PHZ in hexane (the ratio I_E/I_M, the overall shape of the monomer and excimer

fluorescence decays, the first preexponential factor a_{M1} for the monomer decays, the ratio $(a_{E1}/(a_{E2} + a_{E3}))$, and the quantity $((\tau_M/\langle\tau\rangle) - 1)(\eta/\tau_M))$ indicate that this oligomer/solvent system behaves in a unique manner. However the labeling reaction of OIB−MA with PHZ to yield OIB−PHZ was shown not to be complete. Thus, some MA moieties remain unreacted after the pyrene labeling reaction and could be hydrolyzed over time into carboxylic acids, which could induce associations in hexane via the formation of hydrogen bonds.[16] To check whether the presence of carboxylic acid functions was responsible for inducing aggregation of the OIB−PHZ sample in hexane, two experiments were carried out.

First the OIB−PHZ was methylated, so that all carboxylic acids which could potentially promote polar associations via hydrogen bonding, are transformed into methyl esters, which cannot form hydrogen bonds. The extent of methylation reaction was determined by ^{1}H NMR. UV/vis absorption measurements demonstrated that the methylation reaction did not affect the pyrene labeling of the OIB−PHZ sample. Steady-state and time-resolved fluorescence experiments were also carried out with the methylated sample. The results are the circles filled in gray shown in Figures 3 and 5−9. Within experimental error, all fluorescence measurements carried out with the methylated OIB−PHZ sample in hexane agreed perfectly with those obtained with the nonmethylated OIB−PHZ sample.

Second the pyrene labeling reaction was carried out with a large excess of modified oligomer OIB−MA so that the pyrene content would be only 1.1×10^{-4}mol/g, much lower than the nonmethylated sample investigated in this work which had a pyrene content of 2.6×10^{-4}mol/g. The sample containing less pyrene is expected to display more carboxylic acid functions. Nevertheless all the features described for the high pyrene content samples were also observed with the OIB−PHZ sample, which contained less pyrene (data not shown).

At this stage, our fluorescence data have established that OIB−PHZ associates strongly in hexane, OIB−PMA is partially associated in hexane, OIB−PMA and OIB−PHZ are not associated in THF, and the strong association exhibited by OIB−PHZ in hexane is not due to the presence of unreacted MA moieties. To characterize quantitatively the association level of these different oligomeric systems, the fractions of groups, which are associated and unassociated, must be determined. Since pyrene has been attached onto the associating groups and since pyrene responds differently whether it is involved into a pyrene aggregate or whether it is acting as a single unit, a thorough analysis of the fluorescence data should yield the fractions of pyrenes, which are associated or unassociated. This task is attempted in the following section.

Discussion

To describe quantitatively the association level of these oligomeric systems, models are derived in this section which try to account for the various features observed in the fluorescence data. The fluorescence decays obtained for the monomer and excimer of OIB−PMA in hexane are very similar to those obtained for both OIB−Pys in THF. Consequently their fluorescence decays were analyzed in the same manner according to Scheme 3.

Scheme 3 acknowledges the fact that several pyrene groups can be attached onto a single OIB chain. These pyrene groups are referred to as Py_{agg}. The notation Py refers to single pyrene groups attached onto one OIB chain. Upon excitation, the excited Py* can form an excimer by either encountering a ground state Py or Py_{agg}. Both species Py and Py_{agg} act as a quencher and are referred to as *Q* in Scheme 3. The rate constant of intermolecular excimer formation is given by k_{EM}, whereas the rate constant of intramolecular excimer formation is given by k_{agg}. An excimer formed intermolecularly from Py* or intramolecularly from Py_{agg}* undergoes dissociation with a rate constant k_{ME} or k_{-agg}, respectively.

Several steps were taken in order to carry out the analysis of the fluorescence decays according to Scheme 3. The pyrene excimer has usually a small dissociation constant.[6] To limit the number of unknown parameters, k_{-agg} was set to equal zero in Scheme 3, because the already slow dissociation process was expected to be even slower for two pyrenes attached on the same OIB chain. In a first attempt, the rate constant k_{agg} was assumed to be too large to be detected by our time-resolved spectrofluorometer. With this assumption, two and three exponentials are expected to fit the monomer and excimer decays, respectively. Simultaneous analysis of the monomer and excimer fluorescence decays according to these assumptions yielded χ^2 larger than 1.30, indicating poor fits, and the residuals were distorted at the early times. Such behavior could be the consequence of some rapid processes occurring at the early times, such as intramolecular excimer formation. Consequently k_{agg} was assumed to be large, but not so large that our instrument could not detect it. The monomer and excimer fluorescence decays were fitted simultaneously by eqs 3 and 4, respectively. The derivation of eqs 3 and 4 is given in Appendix A. The decay times and preexponential factors retrieved from the analysis of OIB−PMA in THF, OIB−PHZ in THF, and OIB−PMA in hexane are listed in Table 3, parts A−C, respectively. The χ^2 parameters were all smaller than 1.30; the residuals and the autocorrelation function of the residuals were randomly distributed around zero, indicating good fits (cf. Figure 4).

In eqs 3 and 4, the two first exponentials deal with excimer formation via intermolecular diffusion-controlled processes. They can be analyzed according to Birks' scheme formalism (cf. eqs A18−A23) and they yield the values of $k_{EM}[Q]$, k_{ME} and τ_E, which are listed in Table 4, parts A−C). Since the parameter $k_{EM}[Q]$ describes the process of excimer formation via diffusion, it must be corrected for the viscosity change of the oligomer solution. This is done by multiplying the product $k_{EM}[Q]$ by the viscosity η. The difference in pyrene content between OIB−PMA and OIB−PHZ was taken into account by plotting the product $\eta k_{EM}[Q]$ as a function of pyrene concentration, as shown in Figure 8. According to Scheme 3, a plot of $\eta k_{EM}[Q]$ vs pyrene concentration should yield a straight line. This is indeed observed for both OIB−Pys in THF and OIB−PMA in hexane, which behave in an identical manner. It is also interesting to note that the slope of this straight line, which is an estimate of the product ηk_{EM}, yields a value of 760 ± 25 kPa·L·mol^{-1}, surprisingly close to the 780 ± 50 kPa·L·mol^{-1} value obtained for ηk_Q in Figure 7.

As expected for the pyrene excimer, a small dissociation rate constant k_{ME} of $(1.0 \pm 0.2) \times 10^6$, $(1.2 \pm 0.4) \times 10^6$, and $(1.0 \pm 0.7) \times 10^6$ s^{-1} was retrieved for OIB−PMA in THF, OIB−PHZ in THF, and OIB−PMA in

Table 3. Decay Times and Preexponential Factors Obtained from the Fit of the Fluorescence Decays of OIB−PMA and OIB−PHZ in THF and Hexane with Eqs 3 and 4

[OIB] (g/L)	$\tau_{1(ns)}$	$\tau_{2\,(ns)}$	$\tau_{3\,(ns)}$	a_{M1}	a_{M2}	a_{M3}	a_{E1}	a_{E3}	a_{E4}	χ^2
A. OIB−PMA in THF										
26	43 ± 1	91 ± 0	9.4 ± 0.7	0.14 ± 0.01	0.71 ± 0.01	0.15 ± 0.01	−1.00	−0.07 ± 0.01	0.28 ± 0.00	1.27
45	44 ± 1	66 ± 0	10 ± 1	0.31 ± 0.02	0.54 ± 0.01	0.16 ± 0.01	−1.00	−0.05 ± 0.00	0.16 ± 0.00	1.14
67	37 ± 0	57 ± 0	5.4 ± 0.3	0.56 ± 0.01	0.29 ± 0.00	0.15 ± 0.01	−1.00	−0.04 ± 0.00	0.14 ± 0.00	1.08
119	27 ± 1	44 ± 1	14 ± 1	0.71 ± 0.01	0.06 ± 0.01	0.23 ± 0.02	−1.00	−0.25 ± 0.02	0.39 ± 0.03	1.13
134	25 ±1	44 ± 1	9.6 ± 2.0	0.77 ± 0.08	0.05 ± 0.01	0.18 ± 0.8	−1.00	−0.06 ± 0.06	0.19 ± 0.06	1.17
163	23 ± 0	42 ± 0	8.5 ± 0.6	0.77 ± 0.01	0.06 ± 0.03	0.17 ± 0.02	−1.00	−0.07 ± 0.01	0.22 ± 0.01	1.00
B. OIB−PHZ in THF										
49	42 ± 1	70 ± 0	14 ± 3	0.25 ± 0.04	0.66 ± 0.02	0.09 ± 0.02	−1.00	−0.03 ± 0.01	0.15 ± 0.01	1.16
75	40 ± 1	56 ± 1	18 ± 2	0.45 ± 0.04	0.40 ± 0.01	0.15 ± 0.03	−1.00	−0.04 ± 0.01	0.13 ± 0.01	1.14
110	30 ± 0	51 ± 0	9.1 ± 0.7	0.70 ± 0.01	0.15 ± 0.00	0.14 ± 0.01	−1.00	−0.05 ± 0.01	0.16 ± 0.01	1.04
145	28 ± 1	50 ± 0	12 ± 1	0.73 ± 0.02	0.13 ± 0.01	0.14 ± 0.03	−1.00	−0.07 ± 0.02	0.20 ± 0.02	1.06
C. OIB−PMA in Hexane										
8	44 ± 1	114 ± 0	14 ± 2	0.09 ± 0.02	0.77 ± 0.01	0.14 ± 0.01	−1.00	−0.05 ± 0.01	0.42 ± 0.01	1.26
12	48 ± 2	91 ± 1	24 ± 3	0.02 ± 0.07	0.79 ± 0.03	0.19 ± 0.04	−1.00	−0.08 ± 0.04	0.34 ± 0.04	1.23
27	44 ± 1	54 ± 1	16 ± 1	0.55 ± 0.03	0.23 ± 0.04	0.23 ± 0.01	−1.00	−0.03 ± 0.01	0.12 ± 0.02	1.06
53	27 ± 0	54 ± 0	6.7 ± 0.3	0.75 ± 0.00	0.06 ± 0.00	0.19 ± 0.01	−1.00	−0.08 ± 0.01	0.34 ± 0.01	1.22
63	24 ± 0	54 ± 0	8.6 ± 0.8	0.79 ± 0.02	0.05 ± 0.00	0.16 ± 0.02	−1.00	−0.05 ± 0.01	0.36 ± 0.01	1.01
120	18 ± 0	46 ± 0	4.9 ± 0.3	0.75 ± 0.01	0.06 ± 0.00	0.19 ± 0.01	−1.00	−0.11 ± 0.01	0.68 ± 0.02	1.17
160	17 ± 0	42 ± 0	8.7 ± 0.3	0.62 ± 0.02	0.03 ± 0.01	0.35 ± 0.02	−1.00	−0.30 ± 0.04	1.02 ± 0.06	1.03

Table 4. Kinetic Parameters Obtained from the Analysis of OIB−PMA, OIB−PHZ, and PMA-Labeled OIB in THF and Hexane According to Scheme 3

[OIB] (g/L)	k_{agg} (10^7 s^{-1})	k_{EM}[Q] (10^7 s^{-1})	k_{ME} (10^7 s^{-1})	τ_E (ns)
A. OIB−PMA in THF				
26	10.3 ± 0.8	1.0 ± 0.0	0.21 ± 0.00	53 ± 1
45	9.3 ± 0.5	1.4 ± 0.0	0.10 ± 0.00	53 ± 0
67	18.3 ± 1.0	2.0 ± 0.0	0.11 ± 0.00	51 ± 0
119	7.0 ± 0.3	3.3 ± 0.1	0.05 ± 0.00	43 ± 0
134	10.1 ± 1.3	3.5 ± 0.1	0.05 ± 0.00	43 ± 1
163	11.4 ± 0.8	3.9 ± 0.1	0.07 ± 0.00	41 ± 0
B. OIB−PHZ in THF				
49	6.9 ± 1.2	1.2 ± 0.0	0.15 ± 0.00	51 ± 1
75	5.2 ± 0.7	1.7 ± 0.1	0.07 ± 0.01	49 ± 0
110	10.5 ± 0.8	2.6 ± 0.0	0.10 ± 0.00	47 ± 0
145	8.2 ± 0.9	2.8 ± 0.1	0.11 ± 0.01	47 ± 0
C. PMA-Labeled OIB in Hexane				
8	6.9 ± 0.9	0.7 ± 0.0	0.23 ± 0.02	53 ± 2
12[a]	n.a.	n.a.	n.a.	n.a.
27	6.0 ± 0.3	1.9 ± 0.0	0.02 ± 0.00	51 ± 0
53	14.7 ± 0.7	3.3 ± 0.0	0.07 ± 0.00	52 ± 0
63	11.4 ± 0.1	3.7 ± 0.0	0.07 ± 0.00	53 ± 0
120	20.0 ± 1.0	4.9 ± 0.0	0.14 ± 0.00	44 ± 0
160	11.2 ± 0.4	5.6 ± 0.1	0.11 ± 0.00	41 ± 0

[a] Error in a_{M1} listed in Table 3c is too large to yield reliable kinetic parameters.

hexane, respectively. Over the concentration range studied, the excimer lifetime takes a value of 47 ± 5, 47 ± 3, and 49 ± 5 ns for OIB−PMA in THF, OIB−PHZ in THF, and OIB−PMA in hexane, respectively. These values are reasonable for the pyrene excimer.[6] Within experimental error, τ_E takes a value close to 50 ns which justifies our assumption that τ_D equals 50 ns in the analysis of the fluorescence decays.

Since k_{-agg} has been set to equal zero in Scheme 3, the third decay time yields the rate constant of intramolecular excimer formation k_{agg} (cf. eq A24). k_{agg} was found to equal (1.1 ± 0.4) × 10^8, (0.8 ± 0.2) × 10^8, and (1.1 ± 0.6) × 10^8 s^{-1} for OIB−PMA in THF, OIB−PHZ in THF, and OIB−PMA in hexane, respectively. The rate constant of intramolecular excimer formation was the largest rate constant retrieved from this analysis, as expected for excimer formation inside a pyrene aggregate.

The fraction of pyrenes (f_{agg}), which are attached on OIB chains, which display more than one pyrene moiety,

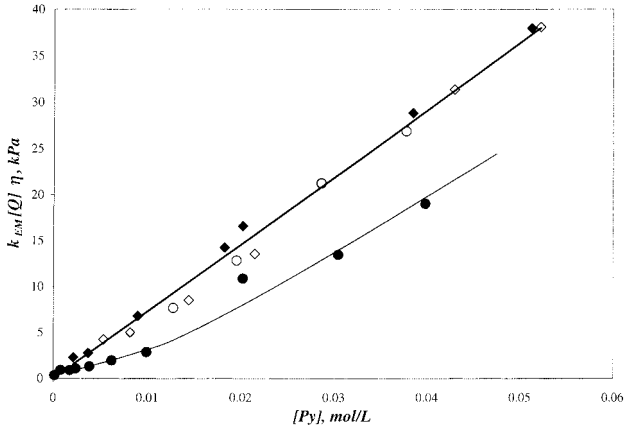

Figure 8. Plot of $k_{EM}[Q]\eta$ vs pyrene concentration for OIB−PMA (pyrene content = 3.3 × 10^{-4} mol/g of oligomer) in THF (◇) and in hexane (◆) and for OIB−PHZ (pyrene content = 2.6 × 10^{-4} mol/g of oligomer) in THF (○) and in hexane (●, nonmethylated sample; gray circle, methylated sample).

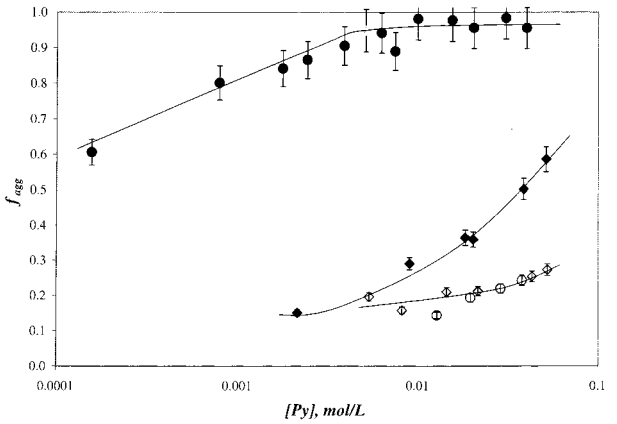

Figure 9. Plot of f_{agg} as a function of pyrene concentration for OIB−PMA (pyrene content = 3.3 × 10^{-4} mol/g of oligomer) in THF (◇) and in hexane (◆) and for OIB−PHZ (pyrene content = 2.6 × 10^{-4} mol/g of oligomer) in THF (○) and in hexane (●, nonmethylated sample; gray circle, methylated sample).

was calculated from eq A26. Figure 9 represents f_{agg} for both OIB−Pys in THF and OIB−PMA in hexane as a function of pyrene concentration. Within experimental

Table 5. Decay Times and Pre-Exponential Factors Obtained from the Fit of the Fluorescence Decays of OIB−PHZ in Hexane According to Eqs 6 and 7

[OIB] (g/L)	τ_1(ns)	τ_2 (ns)	τ_3 (ns)	a_{M1}	a_{M2}	a_{M3}	a_{E1}	a_{E3}	a_{E4}	χ^2
0.6	7.7 ± 0.6	61 ± 0	199 ± 0	0.22 ± 0.01	0.08 ± 0.01	0.70 ± 0.01	−0.15 ± 0.01	0.90 ± 0.00	0.10 ± 0.00	1.05
3.0	8.7 ± 0.4	58 ± 0	146 ± 1	0.36 ± 0.01	0.12 ± 0.01	0.52 ± 0.01	−0.18 ± 0.01	0.92 ± 0.00	0.08 ± 0.00	1.15
6.8	8.6 ± 0.3	60 ± 0	148 ± 1	0.50 ± 0.01	0.12 ± 0.01	0.38 ± 0.01	−0.16 ± 0.01	0.92 ± 0.00	0.08 ± 0.00	1.19
9.3	8.8 ± 0.1	60 ± 0	138 ± 1	0.54 ± 0.00	0.13 ± 0.01	0.33 ± 0.00	−0.17 ± 0.01	0.92 ± 0.00	0.08 ± 0.00	1.16
15	9.2 ± 0.1	60 ± 0	127 ± 1	0.60 ± 0.00	0.13 ± 0.01	0.27 ± 0.00	−0.13 ± 0.01	0.92 ± 0.00	0.08 ± 0.00	1.17
20*	10 ± 0	56 ± 0	101 ± 1	0.61 ± 0.00	0.14 ± 0.01	0.25 ± 0.01	−0.17 ± 0.01	0.89 ± 0.00	0.11 ± 0.00	1.28
24	9.0 ± 0.1	59 ± 0	106 ± 1	0.63 ± 0.00	0.18 ± 0.01	0.18 ± 0.01	−0.10 ± 0.01	0.92 ± 0.00	0.08 ± 0.00	1.17
28[b]	11	58	40	0.66	0.15	0.19	−0.14	0.37	0.63	1.26
38	9.3 ± 0.1	59 ± 1	88 ± 3	0.69 ± 0.00	0.16 ± 0.03	0.16 ± 0.03	−0.10 ± 0.01	0.85 ± 0.04	0.15 ± 0.04	1.23
58[a]	8.1 ± 0.0	63 ± 1	35 ± 3	0.73 ± 0.00	0.20 ± 0.01	0.08 ± 0.01	−0.18 ± 0.01	0.79 ± 0.04	0.21 ± 0.04	1.12
59	8.8 ± 0.6	64 ± 0	30 ± 1	0.71 ± 0.01	0.16 ± 0.00	0.12 ± 0.00	−0.16 ± 0.01	0.82 ± 0.01	0.18 ± 0.01	1.18
78	8.0 ± 0.1	63 ± 0	38 ± 1	0.62 ± 0.00	0.13 ± 0.01	0.25 ± 0.00	−0.13 ± 0.01	0.96 ± 0.02	0.04 ± 0.02	0.95
117	9.4 ± 0.1	63 ± 1	37 ± 2	0.78 ± 0.00	0.10 ± 0.01	0.12 ± 0.00	−0.11 ± 0.01	0.74 ± 0.03	0.26 ± 0.03	1.08
153	8.3 ± 0.1	59 ± 0	31 ± 1	0.72 ± 0.01	0.06 ± 0.00	0.23 ± 0.00	−0.16 ± 0.01	0.84 ± 0.01	0.16 ± 0.01	1.11

[a] Methylated OIB−PHZ sample. [b] This polymer concentration lies in the crossover region and the software cannot converge for some of the simulated decays.

error, f_{agg} for both OIB−Pys in THF is found to remain constant with OIB concentration and equals 0.21 ± 0.04. This indicates that 79% of all MA moieties are present as single units on the OIB and 21% of MA moieties are involved into MA aggregates. These MA aggregates can be either oligoMA or several MA units attached close to one another onto the same OIB chain. This study in THF provides information about the microstructure of OIB−MA. Figure 9 also shows that some aggregation is taking place for OIB−PMA in hexane above a pyrene concentration of 0.01 mol/L since the fraction f_{agg} takes values which are larger than its expected lowest value of 0.21 obtained in THF, where no intermolecular associations are supposed to occur.

Since the monomer and excimer decays of OIB−PHZ in hexane behaved in a very distinct manner due to the presence of pyrene aggregates, they were analyzed according to Scheme 4. In Scheme 4 the pyrene excimer forms in a sequential manner. First OIB−PHZ molecules encounter and form a stable aggregate via polar associations between the MA moieties. In Scheme 4, k_{EM} is the rate constant for diffusional encounters and k_{ME} is the dissociation rate constant of a polar aggregate. The polar aggregates were assumed to be stable during the lifetime of an excited pyrene and k_{ME} was set to equal zero, as was previously done in an earlier work dealing with modified polyolefins in hexane.[12] Inside a polar aggregate, the pyrenes rearrange on a fast time scale to form an excimer with a rate constant k_{agg}. Within the polar aggregate the excimer can dissociate with a rate constant k_{-agg}. According to Scheme 4, three excited species are present in the solution. They are Py^*_{diff}, Py^*_{agg}, and E*, which represent unassociated excited pyrenes, excited pyrenes involved in a polar aggregate, and the pyrene excimer, respectively. Three differential equations describe the time dependence of Py^*_{diff}, Py^*_{agg}, and E*. Their integration given in Appendix B predicts that the monomer and the excimer decays should be fitted with a sum of three exponentials, where the three decay times τ_1, τ_2, and τ_3 are the same in the decays of the monomer and of the excimer. The decay times and preexponential factors retrieved from the simultaneous analysis of the OIB−PHZ fluorescence decays are listed in Table 5. The kinetic parameters were obtained according to the mathematical treatment given in Appendix B and are listed in Table 6.

In Table 5, τ_1 and τ_2 remain constant for all oligomer concentrations and equal 8.9 ± 0.9 and 60.3 ± 2.2 ns, respectively. Thus, τ_1 and τ_2 represent photophysical processes, which are not affected by the pyrene concentration. Since the pyrene aggregates are expected to remain the same regardless of pyrene concentration, the decay times τ_1 and τ_2 are believed to describe photochemical processes, which are taking place inside the pyrene aggregates. The decay time τ_1 being the shortest decay time certainly represents the process of excimer formation inside a pyrene aggregate (k_{agg} in Scheme 4), whereas τ_2, which is typical of the excimer lifetime (τ_E in Scheme 4) must represent the excimer decay. The third decay time τ_3 decreases with increasing oligomer concentration. This is the expected behavior that a decay time would display for a diffusion-controlled process. Thus, τ_3 represents the contribution of the diffusional encounters and yields the product k_{EM}[Q] as shown in Appendix B (cf. eq B6c). Over the whole oligomer concentration range, τ_3 decreases from 199 to 31 ns, whereas τ_2 remains constant and equals 60.3 ± 2.2 ns. Thus, τ_3 crosses over τ_2 as the oligomer concentration decreases so that for a given oligomer concentration, τ_3 equals τ_2. This situation makes the analysis of the decays very difficult in the concentration range where the crossover takes place, which is estimated to occur between 30 and 60 g/L. The decay times τ_3 and τ_2 are too close to be accurately determined by the analysis program. Thus, the decay times τ_3 retrieved in this OIB−PHZ concentration range were not all taken into consideration.

Table 6. Kinetic Parameters Obtained from the Analysis of PHZ-Labeled OIB in Hexane According to Scheme 4

[OIB], g/L	k_{agg} (10^7 s^{-1})	k_{-agg} (10^7 s^{-1})	$k_{EM}[Q]$ (10^7 s^{-1})	τ_E (ns)
0.6	12.0 ± 1.0	0.58 ± 0.1	0.1 ± 0.0	58 ± 0
3.0	10.5 ± 0.5	0.53 ± 0.05	0.3 ± 0.0	56 ± 0
6.8	10.8 ± 0.4	0.36 ± 0.03	0.3 ± 0.0	58 ± 0
9.3	10.6 ± 0.1	0.35 ± 0.03	0.3 ± 0.0	58 ± 0
15	10.2 ± 0.1	0.24 ± 0.02	0.4 ± 0.0	59 ± 0
24	10.5 ± 1.3	0.24 ± 0.03	0.6 ± 0.0	58 ± 0
28[b]	8.2	0.49	2.1	54.8
38	10.1 ± 0.1	0.20 ± 0.03	0.7 ± 0.0	58 ± 1
58[a]	11.3 ± 0.1	0.55 ± 0.03	2.4 ± 0.0	61 ± 1
59	10.6 ± 0.0	0.38 ± 0.02	2.9 ± 0.1	62 ± 0
78	11.8 ± 0.2	0.27 ± 0.02	2.3 ± 0.1	62 ± 0
117	10.1 ± 0.1	0.15 ± 0.01	2.3 ± 0.1	63 ± 1
153	11.5 ± 0.1	0.14 ± 0.01	2.9 ± 0.0	59 ± 0

[a] Methylated OIB−PHZ sample. [b] This polymer concentration lies in the crossover region, and the software cannot converge for some of the simulated decays.

The kinetic parameters used in Scheme 4 were obtained by following the mathematical treatment

described in Appendix B. They are listed in Table 6 and are very similar to those obtained in Table 4. The rate of excimer formation inside a pyrene aggregate k_{agg} is large and equals $(1.1 \pm 0.1) \times 10^8$ s^{-1}. The excimer dissociation rate constant k_{-agg} is small and equals $(0.34 \pm 0.15) \times 10^7$ s^{-1}. The excimer lifetime τ_E is constant for all concentrations and equals 58.6 ± 2.5 ns. The product $k_{EM}[Q]$ increases with oligomer concentration. Only those values obtained for oligomer concentrations of 28, 38, 58, and 59 g/L exhibit some scattering in the $k_{EM}[Q]$ values due to the analysis problems associated with the decay time crossover. To account for the viscosity increase due to increasing oligomer concentrations, the product $k_{EM}[Q]\eta$ for OIB−PHZ in hexane is plotted as a function of oligomer concentration in Figure 8. The trend is again different from those observed for both OIB−Pys in THF and OIB−PMA in hexane. OIB−PHZ associations might be responsible for this discrepancy. When most pyrene groups are involved into pyrene aggregates as for OIB−PHZ in hexane, the pyrene aggregates constitute the most probable quencher for an excited unassociated pyrene. But a pyrene aggregate also pools together several ground-state pyrenes, which would each act as a single quencher were no pyrene aggregate formed. As a result the concentration of quencher decreases, which explains why the product $k_{EM}[Q]\eta$ is smaller for OIB−PHZ in hexane than for any other data set. As explained in Appendix B, the parameter f_{agg} can be determined by analyzing either the monomer or the excimer decays. When calculated by using either set of data, the f_{agg} values showed some differences. The average value is represented in Figure 9 and the error bars indicate the spread of the difference. In Figure 9, the behavior exhibited by f_{agg} indicates that the level of association of OIB−PHZ in hexane is the highest of all other oligomer/solvent systems studied. Above a pyrene concentration of 0.01 mol/L (equivalent to an oligomer concentration of 40 g/L), all OIB−PHZ are aggregated. The aggregates dissociate at lower pyrene concentrations. These conclusions agree qualitatively with the results presented in the previous section.

Conclusions

The associations between the polar moieties of a modified oligoisobutylene were investigated by using fluorescence spectroscopy. The oligoisobutylene was modified by attempting to attach a single MA unit to one of its ends. Two types of amino-compounds labeled with the dye pyrene were then reacted with the MA moiety. The modified oligoisobutylene displayed a MA-to-pyrene linker, made of either one methylene unit for OIB−PMA or one amide bond −NH−CO− and three methylene units for OIB−PHZ. Analysis of the fluorescence decays of both OIB−Pys in THF showed that only 79% of all MA moieties are attached as single units. Whereas both OIB−Pys do not associate in polar THF, OIB−PMA, and OIB−PHZ were shown to associate mildly and strongly in hexane, respectively. The enhanced association observed with OIB−PHZ in hexane is arising from the more polar MA-to-pyrene linker. By developing models to characterize the kinetics of the pyrene monomer and excimer, the associative strength of these different oligomer/solvent systems could be determined quantitatively.

Acknowledgment. The authors thank NSERC and an Imperial Oil University Research Grant for their support of this research, Sergio F. C. R. Santos for helping them with running some of the fluorescence decays, and Deping Chai for initial experiments.

Appendix A

Determination of the Monomer and Excimer Concentration Profiles According to Scheme 3. In Scheme 3, *Q* is the quencher that can be either a ground-state monomer or a pyrene aggregate. The kinetic equations describing Scheme 3 are given by

$$\frac{d[Py^*]}{dt} = -\left(\frac{1}{\tau_M} + k_{EM}[Q]\right)[Py^*] + k_{ME}[E^*] \quad (A1)$$

$$\frac{d[E^*]}{dt} = k_{EM}[Q][Py^*] - \left(k_{ME} + \frac{1}{\tau_E}\right)[E^*] \quad (A2)$$

$$\frac{d[Py^*_{agg}]}{dt} = -\left(\frac{1}{\tau_M} + k_{agg}\right)[Py^*_{agg}] + k_{-agg}[D^*] \quad (A3)$$

$$\frac{d[D^*]}{dt} = k_{agg}[Py^*_{agg}] - \left(k_{-agg} + \frac{1}{\tau_D}\right)[D^*] \quad (A4)$$

Equations A1 and A2 are first solved according to Birks' classical derivation.

$$\frac{d[Py^*]}{dt} = -X[Py^*] + k_{EM}[E^*] \quad (A5)$$

$$\frac{d[E^*]}{dt} = k_{EM}[Q][Py^*] - Y[E^*] \quad (A6)$$

where

$$X = \frac{1}{\tau_M} + k_{EM}[Q] \quad (A7)$$

and

$$Y = k_{ME} + \frac{1}{\tau_E} \quad (A8)$$

Solving eqs A5 and A6 and applying the initial conditions $[Py^*] = [Py^*]_0$, and $[E^*] = 0$, at $t = 0$, one obtains

$$[Py^*] = \frac{[Py^*]_0}{\lambda_2 - \lambda_1}[(\lambda_2 - X)e^{-\lambda_1 t} + (X - \lambda_1)e^{-\lambda_2 t}] \quad (A9)$$

$$[E^*] = \frac{k_{EM}[Q][Py^*]_0}{\lambda_2 - \lambda_1}[e^{-\lambda_1 t} - e^{-\lambda_2 t}] \quad (A10)$$

where

$$\lambda_{1,2} = \frac{(X + Y) \pm \sqrt{(X + Y)^2 - 4\left(X - \frac{1}{\tau_M}\right)\left(Y - \frac{1}{\tau_E}\right)}}{2} \quad (A11)$$

In eqs A9 and A10, $\lambda_1 = (1/\tau_1)$ and $\lambda_2 = (1/\tau_2)$ where τ_1 and τ_2 are the first and second decay times, respectively.

Equations A3 and A4 were resolved by assuming that k_{-agg} is negligible. The concentration profiles of $[Py^*_{agg}]$ and $[D^*]$ are given in eqs A12 and A13.

$$[\mathrm{Py}^*_{\mathrm{agg}}] = [\mathrm{Py}^*_{\mathrm{agg}}]_0 \exp\left(-\left[\frac{1}{\tau_{\mathrm{M}}} + k_{\mathrm{agg}}\right]t\right) \quad \text{(A12)}$$

$$[D^*] = -\frac{k_{\mathrm{agg}}[\mathrm{Py}_{\mathrm{agg}}]_0}{\frac{1}{\tau_{\mathrm{M}}} - \frac{1}{\tau_D} + k_{\mathrm{agg}}} \exp\left(-\left[\frac{1}{\tau_{\mathrm{M}}} + k_{\mathrm{agg}}\right]t\right) + \left([D^*]_0 + \frac{k_{\mathrm{agg}}[\mathrm{Py}_{\mathrm{agg}}]_0}{\frac{1}{\tau_{\mathrm{M}}} - \frac{1}{\tau_D} + k_{\mathrm{agg}}}\right) \exp\left(-\frac{t}{\tau_D}\right) \quad \text{(A13)}$$

Combining eqs A9 with A12 and A10 with A13 yields the concentration profiles of the pyrene monomer $[\mathrm{Py}^*]_{\mathrm{T}}$ and excimer $[\mathrm{E}^*]_{\mathrm{T}}$, repectively.

$$[\mathrm{Py}^*]_{\mathrm{T}} = \frac{[\mathrm{Py}^*]_0}{\lambda_2 - \lambda_1}[(\lambda_2 - X)\mathrm{e}^{-\lambda_1 t} + (X - \lambda_1)\mathrm{e}^{-\lambda_2 t}] + [\mathrm{Py}^*_{\mathrm{agg}}]_0 \exp\left(-\left[\frac{1}{\tau_{\mathrm{M}}} + k_{\mathrm{agg}}\right]t\right) \quad \text{(A14)}$$

$$[\mathrm{E}^*]_{\mathrm{T}} = \frac{k_{\mathrm{EM}}[\mathrm{Q}][\mathrm{Py}^*]_0}{\lambda_2 - \lambda_1}[\mathrm{e}^{-\lambda_1 t} - \mathrm{e}^{-\lambda_2 t}] - \frac{k_{\mathrm{agg}}[\mathrm{Py}_{\mathrm{agg}}]_0}{\frac{1}{\tau_{\mathrm{M}}} - \frac{1}{\tau_D} + k_{\mathrm{agg}}} \exp\left(-\left[\frac{1}{\tau_{\mathrm{M}}} + k_{\mathrm{agg}}\right]t\right) + \left([D^*]_0 + \frac{k_{\mathrm{agg}}[\mathrm{Py}_{\mathrm{agg}}]_0}{\frac{1}{\tau_{\mathrm{M}}} - \frac{1}{\tau_D} + k_{\mathrm{agg}}}\right) \exp\left(-\frac{t}{\tau_D}\right) \quad \text{(15)}$$

According to eqs A14 and A15, the monomer and excimer decays are represented by three and four exponentials, respectively. The three first decay times in the excimer decay are the same as in the monomer decay. Consequently, the fluorescence intensities of the monomer ($i_{\mathrm{M}}(t)$) and excimer ($i_{\mathrm{E}}(t)$) can be written as

$$i_{\mathrm{M}}(t) = a_{\mathrm{M1}} \exp(-t/\tau_1) + a_{\mathrm{M2}} \exp(-t/\tau_2) + a_{\mathrm{M3}} \exp(-t/\tau_3) \quad \text{(A16)}$$

$$i_{\mathrm{E}}(t) = a_{\mathrm{E1}} \exp(-t/\tau_1) + a_{\mathrm{E2}} \exp(-t/\tau_2) + a_{\mathrm{E3}} \exp(-t/\tau_3) + a_{\mathrm{E4}} \exp(-t/\tau_{\mathrm{D}}) \quad \text{(A17)}$$

Determination of the Rate Parameters. The kinetic parameters $k_{\mathrm{EM}}[\mathrm{Q}]$, k_{ME}, and τ_{E} in Scheme 3 were obtained by handling the two first exponentials in eqs A14 and A15 in the same manner as the Birks' treatment.

$$A = \frac{a_{\mathrm{M2}}}{a_{\mathrm{M1}}} \quad \text{(A18)}$$

$$X = \frac{(A\lambda_2 + \lambda_1)}{(A + 1)} \quad \text{(A19)}$$

$$k_{\mathrm{EM}}[\mathrm{Q}] = X - \frac{1}{\tau_{\mathrm{M}}} \quad \text{(A20)}$$

$$Y = \lambda_2 + \lambda_1 - X \quad \text{(A21)}$$

$$k_{\mathrm{ME}} = \frac{(X - \lambda_1)(\lambda_2 - X)}{k_{\mathrm{EM}}[\mathrm{Q}]} \quad \text{(A22)}$$

$$k_{\mathrm{E}} = \frac{1}{\tau_{\mathrm{E}}} = Y - k_{\mathrm{ME}} \quad \text{(A23)}$$

In eqs A16 and A17, τ_3 yields the rate of excimer formation inside a pyrene aggregate.

$$k_{\mathrm{agg}} = \frac{1}{\tau_3} - \frac{1}{\tau_{\mathrm{M}}} \quad \text{(A24)}$$

The fraction of pyrenes (f_{agg}), which are attached on OIB chains displaying more than one MA moiety, is given by eq A25

$$f_{\mathrm{agg}} = \frac{[\mathrm{Py}^*_{\mathrm{agg}}]_0 + [\mathrm{D}^*]_0}{[\mathrm{Py}^*]_0 + [\mathrm{Py}^*_{\mathrm{agg}}]_0 + [\mathrm{D}^*]_0} \quad \text{(A25)}$$

where the concentrations $[\mathrm{Py}^*]_0$, $[\mathrm{Py}^*_{\mathrm{agg}}]_0$, and $[\mathrm{D}^*]_0$ are functions of the $a_{\mathrm{M}i}$ and $a_{\mathrm{E}i}$ preexponential factors with $i = 1-3$. Fitting the fluorescence decays with eqs A16 and A17 yielded a very small a_{E3} coefficient (cf. Table 3), which suggested that this parameter is retrieved with some uncertainty. Consequently, f_{agg} was calculated by re-arranging the preexponential factors a_{M1}, a_{M3}, a_{E1}, and a_{E4} in eqs A16 and A17 and the preexponential factor a_{E3} was kept out of the derivation.

$$f_{\mathrm{agg}} = 1 - \left(1 + \frac{k_{\mathrm{EM}}[\mathrm{Q}]}{\lambda_2 - \lambda_1} \times \frac{a_{\mathrm{E4}}}{a_{\mathrm{E1}}} + \left(1 - \frac{k_{\mathrm{agg}}}{\frac{1}{\tau_{\mathrm{M}}} - \frac{1}{\tau_{\mathrm{E}}} + k_{\mathrm{agg}}}\right) \times \frac{\lambda_2 - X}{\lambda_2 - \lambda_1} \times \frac{a_{\mathrm{M3}}}{a_{\mathrm{M1}}}\right)^{-1} \quad \text{(A26)}$$

Appendix B

Determination of the Monomer and Excimer Concentration Profiles According to Scheme 4. In Scheme 4, an unassociated excited pyrene ($\mathrm{Py}^*_{\mathrm{diff}}$) can either emit a photon with its own fluorescence lifetime τ_{M} or it can encounter a quencher, which is either an unassociated ground-state pyrene (GSPy), a GSPy attached onto oligoMA, or a GSPy located inside a polar aggregate. The net result of this encounter is the formation of a pyrene aggregate containing one excited pyrene ($\mathrm{Py}^*_{\mathrm{agg}}$). The rate of diffusional encounter is given as $k_{\mathrm{EM}}[\mathrm{Q}]$ where [Q] represents the concentration of quencher species which can associate with $\mathrm{Py}^*_{\mathrm{diff}}$. Upon a rapid rearrangement occurring with a pseudo-unimolecular rate constant k_{agg}, $\mathrm{Py}^*_{\mathrm{agg}}$ can form an excimer E*. The excimer can either fluoresce with a lifetime τ_{E} or dissociate to give back $\mathrm{Py}^*_{\mathrm{agg}}$ with a rate constant $k_{-\mathrm{agg}}$.

According to Scheme 4, the time dependence of the three species is described by the three following differential equations:

$$\frac{[\mathrm{Py}^*_{\mathrm{diff}}]}{\mathrm{d}t} = -\left(k_{\mathrm{EM}}[\mathrm{Q}] + \frac{1}{\tau_{\mathrm{M}}}\right)[\mathrm{Py}^*_{\mathrm{diff}}] \quad \text{(B1)}$$

$$\frac{\mathrm{d}[\mathrm{Py}^*_{\mathrm{agg}}]}{\mathrm{d}t} = k_{\mathrm{EM}}[\mathrm{Q}][\mathrm{Py}^*_{\mathrm{diff}}] - \left(k_{\mathrm{agg}} + \frac{1}{\tau_{\mathrm{M}}}\right)[\mathrm{Py}^*_{\mathrm{agg}}] + k_{-\mathrm{agg}}[\mathrm{E}^*] \quad \text{(B2)}$$

$$\frac{\mathrm{d}[\mathrm{E}^*]}{\mathrm{d}t} = k_{\mathrm{agg}}[\mathrm{Py}^*_{\mathrm{agg}}] - \left(k_{-\mathrm{agg}} + \frac{1}{\tau_{\mathrm{E}}}\right)[\mathrm{E}^*] \quad \text{(B3)}$$

Integration of this set of differential equations yields two triexponential functions for the concentration of the excited pyrene monomer ($[Py^*]_T$) and the pyrene excimer concentration ($[E^*]$) where the three decay times are the same in both expressions as shown in eqs B4 and B5.

$$[Py^*]_T = [Py^*_{diff}] + [Py^*_{agg}] = a_{M1}\, e^{-t/\tau_1} + a_{M2}\, e^{-t/\tau_2} + a_{M3}\, e^{-t/\tau_3} \quad \text{(B4)}$$

$$[E^*] = a_{E1}\, e^{-t/\tau_1} + a_{E2}\, e^{-t/\tau_2} + a_{E3}\, e^{-t/\tau_3} \quad \text{(B5)}$$

The expressions of the decay times and preexponential factors given as a function of the parameters $k_{EM}[Q]$, k_{agg}, k_{-agg}, τ_M, τ_E, $[Py^*_{diff}]_0$ (which equals $[Py^*_{diff}]$ at time $t = 0$), $[Py^*_{agg}]_0$ (which equals $[Py^*_{agg}]$ at time $t = 0$), and $[E^*]_0$ (which equals $[E^*]_0$ at time $t = 0$) have been derived hereafter by using the following notations:

$$X_0 = k_{EM}[Q] + \frac{1}{\tau_M} \quad X = k_{agg} + \frac{1}{\tau_M} \quad Y = k_{-agg} + \frac{1}{\tau_E}$$

The decay times τ_1, τ_2, and τ_3 are given in eq B6a−c.

$$-\frac{1}{\tau_1} = \frac{-(X+Y) - \sqrt{(X+Y)^2 - 4\left(X - \frac{1}{\tau_M}\right)\left(Y - \frac{1}{\tau_E}\right)}}{2} \quad \text{(B6a)}$$

$$-\frac{1}{\tau_2} = \frac{-(X+Y) + \sqrt{(X+Y)^2 - 4\left(X - \frac{1}{\tau_M}\right)\left(Y - \frac{1}{\tau_E}\right)}}{2} \quad \text{(B6b)}$$

$$\frac{1}{\tau_3} = X_0 = k_{EM}[Q] + \frac{1}{\tau_M} \quad \text{(B6c)}$$

According to eq B6c, τ_3 decreases with increasing oligomer concentration. The expressions of τ_1 and τ_2 depend only on k_{agg}, k_{-agg}, τ_M, and τ_E. Since k_{agg} and k_{-agg} characterize the polar aggregates, which are assumed to preserve their features over the covered range of oligomer concentration, τ_1 and τ_2 are not supposed to change with oligomer concentration, whereas τ_3 does. These conclusions agree well with our experimental observations.

The expressions of the a_{Mi} and a_{Ei} preexponential factors are shown in eqs B7a−c and B8a−c, respectively.

$$a_{M1} = \frac{Y - \frac{1}{\tau_1}}{X - \frac{1}{\tau_M}} a_{E1} \quad \text{(B7a)}$$

$$a_{M2} = \frac{Y - \frac{1}{\tau_2}}{X - \frac{1}{\tau_M}} a_{E2} \quad \text{(B7b)}$$

$$a_{M3} = \frac{Y - \frac{1}{\tau_3}}{X - \frac{1}{\tau_M}} a_{E3} + [Py^*_{diff}]_0 \quad \text{(B7c)}$$

$$a_{E1} = \frac{\left(Y - \frac{1}{\tau_2}\right)[E^*]_0 - \left(X - \frac{1}{\tau_M}\right)[Py^*_{agg}]_0 - \nu[Py^*_{diff}]_0\left(\frac{1}{\tau_3} - \frac{1}{\tau_2}\right)}{\frac{1}{\tau_1} - \frac{1}{\tau_2}} \quad \text{(B8a)}$$

$$a_{E2} = \frac{\left(Y - \frac{1}{\tau_1}\right)[E^*]_0 - \left(X - \frac{1}{\tau_M}\right)[Py^*_{agg}]_0 - \nu[Py^*_{diff}]_0\left(\frac{1}{\tau_3} - \frac{1}{\tau_1}\right)}{\frac{1}{\tau_2} - \frac{1}{\tau_1}} \quad \text{(B8b)}$$

$$a_{E3} = \frac{\left(X_0 + \frac{1}{\tau_M}\right)\left(X - \frac{1}{\tau_M}\right)}{X_0^2 - X_0(X+Y) + X\,Y - \left(Y - \frac{1}{\tau_E}\right)\left(X - \frac{1}{\tau_M}\right)}[Py^*_{diff}]_0 = \nu[Py^*_{diff}]_0 \quad \text{(B8c)}$$

The origin of the ν coefficient used in eqs B8a and B8b is given in eq B8c.

Determination of the Rate Parameters and the Fraction of Associated Pyrenes. The first section of Appendix B showed that, according to Scheme 4, the fluorescence decays of the pyrene monomer and excimer are expected to exhibit triexponential decays. Expressions of the preexponential factors and decay times were given as a function of the rate constants and concentrations at initial time. Now the reverse operation is being carried out where the expressions of the parameters $k_{EM}[Q]$, k_{agg}, k_{-agg}, τ_M, τ_E, $[Py^*_{diff}]_0$, $[Py^*_{agg}]_0$, and $[E^*]_0$ are obtained as a function of the preexponential factors and the decay times. The rate constants were determined according to the following procedure.

$$A = \frac{a_{M1}/a_{E1}}{a_{M2}/a_{E2}} \quad \text{(B9)}$$

$$Y = \frac{\frac{A}{\tau_2} - \frac{1}{\tau_1}}{A - 1} \quad \text{(B10)}$$

$$X = \frac{1}{\tau_1} + \frac{1}{\tau_2} - Y \quad \text{(B11)}$$

$$k_{agg} = X - \frac{1}{\tau_M} \quad \text{(B12)}$$

$$k_{-agg} = \frac{X\,Y - \frac{1}{\tau_1}\frac{1}{\tau_2}}{k_{agg}} \quad \text{(B13)}$$

$$\tau_E = (Y - k_{-agg})^{-1} \quad \text{(B14)}$$

$$k_{diff}[Q] = X_0 - \frac{1}{\tau_M} \quad \text{(B15)}$$

The fractions of unassociated pyrenes (f_{diff}) and of associated pyrenes (f_{agg}) can be calculated from the monomer decays or from the excimer decays. First the parameter ν is calculated according to eq B16:

$$\nu = \frac{\left(X_0 + \frac{1}{\tau_M}\right)\left(X - \frac{1}{\tau_M}\right)}{{X_0}^2 - X_0(X + Y) + X\,Y - \left(X - \frac{1}{\tau_M}\right)\left(Y - \frac{1}{\tau_E}\right)} \quad \text{(B16)}$$

From the Excimer Decays:

$$f_{diff} = \frac{[Py^*_{diff}]_0}{[Py^*_{diff}] + [Py^*_{agg}]_0 + [E^*]_0} =$$

$$\frac{1}{1 + \nu\frac{a_{E1}}{a_{E3}}\left(1 + \frac{Y - \frac{1}{\tau_1}}{X - \frac{1}{\tau_M}}\right) + \nu\frac{a_{E2}}{a_{E3}}\left(1 + \frac{Y - \frac{1}{\tau_2}}{X - \frac{1}{\tau_M}}\right) + \nu\left(1 + \frac{Y - \frac{1}{\tau_3}}{X - \frac{1}{\tau_M}}\right)} \quad \text{(B17a)}$$

$$\frac{[Py^*_{agg}]_0}{[Py^*_{diff}]_0 + [Py^*_{agg}]_0 + [E^*]_0} = f_{diff}\left[\frac{a_{E1}}{a_{E3}}\left(Y - \frac{1}{\tau_1}\right) + \frac{a_{E2}}{a_{E3}}\left(Y - \frac{1}{\tau_2}\right) + \left(Y - \frac{1}{\tau_3}\right)\right] \times \frac{\nu}{X - \frac{1}{\tau_M}} \quad \text{(B17b)}$$

$$\frac{[E^*]_0}{[Py^*_{diff}]_0 + [Py^*_{agg}]_0 + [E^*]_0} = f_{diff}\left(\frac{a_{E1}}{a_{E3}} + \frac{a_{E2}}{a_{E3}} + 1\right)\nu \quad \text{(B17c)}$$

and

$$f_{agg} = 1 - f_{diff} = \frac{[Py^*_{agg}]_0 + [E^*]_0}{[Py^*_{diff}]_0 + [Py^*_{agg}]_0 + [E^*]_0} \quad \text{(B17d)}$$

From the Monomer Decays:

$$f_{diff} = \frac{[Py^*_{diff}]_0}{[Py^*_{diff}]_0 + [Py^*_{agg}]_0 + [E^*]_0} =$$

$$\frac{1}{\left(1 + \nu\frac{Y - \frac{1}{\tau_3}}{X - \frac{1}{\tau_M}}\right)\left[1 + \frac{a_{M1}}{a_{M3}}\left(1 + \frac{X - \frac{1}{\tau_M}}{Y - \frac{1}{\tau_1}}\right) + \frac{a_{M2}}{a_{M3}}\left(1 + \frac{X - \frac{1}{\tau_M}}{Y - \frac{1}{\tau_2}}\right)\right] + \nu} \quad \text{(B18a)}$$

$$\frac{[Py^*_{agg}]_0}{[Py^*_{diff}]_0 + [Py^*_{agg}]_0 + [E^*]_0} = f_{diff}\left[\left(\frac{a_{M1}}{a_{M3}} + \frac{a_{M2}}{a_{M3}}\right)\left(1 + \nu\frac{Y - \frac{1}{\tau_3}}{X - \frac{1}{\tau_M}}\right) + \nu\frac{Y - \frac{1}{\tau_3}}{X - \frac{1}{\tau_M}}\right] \quad \text{(B18b)}$$

$$\frac{[E^*]_0}{[Py^*_{diff}]_0 + [Py^*_{agg}]_0 + [E^*]_0} = f_{diff}\left[\left(\frac{a_{M1}}{a_{M3}}\frac{X - \frac{1}{\tau_M}}{Y - \frac{1}{\tau_1}} + \frac{a_{M2}}{a_{M3}}\frac{X - \frac{1}{\tau_M}}{Y - \frac{1}{\tau_2}}\right)\left(1 + \nu\frac{Y - \frac{1}{\tau_3}}{X - \frac{1}{\tau_M}}\right) + \nu\right] \quad \text{(B18c)}$$

and

$$f_{agg} = 1 - f_{diff} = \frac{[Py^*_{agg}]_0 + [E^*]_0}{[Py^*_{diff}]_0 + [Py^*_{agg}]_0 + [E^*]_0} \quad \text{(B18d)}$$

References and Notes

(1) Glass, J. E. *Hydrophilic Polymers. Performance with Environmental Acceptability*; Advances in Chemistry Series 248; American Chemical Society. Washington, DC, 1996. Schulz, D. N.; Glass, J. E. *Polymers as Rheology Modifiers*; ACS Symposium Series 462; American Chemical Society. Washington, DC, 1989.

(2) Jenkins, R. D.; Bassett, D. R.; Silebi, C. A.; El-Aasser, M. S. *J. Appl. Polym. Sci.* **1995**, *58*, 209−230. Regalado, E. J.; Selb, J.; Candau, F. *Macromolecules* **1999**, *32*, 8580−8588.

(3) Jenkins, R. D.; Sinha, B. R.; Bassett, D. R. *Polym. Mater. Sci. Eng.* **1991**, *65*, 72.

(4) Annabale, T.; Buscall, R.; Rammile, E.; Whittlestone, D. *J. Rheol.* **1993**, *37*, 695−726. Volpert, E.; Selb, J.; Candau, F. *Macromolecules* **1996**, *29*, 1452−1463.

(5) Tanaka, F.; Edwards, S. F. *Macromolecules* **1992**, *25*, 1516−1523. Semenov, A. N.; Joanny, J.-F.; Khokhlov, A. R. *Macromolecules* **1995**, *28*, 1066−1075.

(6) Birks, J. B. *Photophysics of Aromatic Molecules*; Wiley: New York, 1970; pp 301−371.

(7) Ringsdorf, H.; Venzmer, J.; Winnik, F. M. *Angew. Chem., Int. Ed. Engl.* **1991**, *30*, 315−318. Kramer, M. C.; Welch, Steger, J. R.; McCormick, C. L. *Macromolecules* **1995**, *28*, 5248−5254. Mizusaki, M.; Morishima, Y.; Winnik, F. M. *Macromolecules* **1999**, *32*, 4317−4326.

(8) Ebata, K.; Masuko, M.; Ohtani, H.; Kashiwasake-Jibu, M. *Photochem. Photobiol.* **1995**, *62*, 836−839.

(9) Mathew, A. K.; Siu, H.; Duhamel, J. *Macromolecules* **1999**, *32*, 7100−7108.

(10) Winnik, F. M. *Chem. Res.* **1993**, *93*, 587−614 and references herein.

(11) Covitch, M. J. *The Lubrizol Corporation* **1999**, *01*, 3463. Jao, T.-C.; Mishra, M. K.; Rubin, I. D.; Duhamel, J.; Winnik, M. A. *J. Polym. Sci., Part B: Polym. Phys.* **1995**, *33*, 1173−1181. Mishra, M. K.; Rubin, I. D. US Patent 5,200,102, 1993.

(12) Vangani, V.; Duhamel, J.; Nemeth, S.; Jao, T.-C. *Macromolecules* **1999**, *32*, 2845−2854.

(13) Nemeth, S.; Jao, T.-C.; Fendler, J. *Macromolecules* **1994**, *27*, 5449−5456.

(14) Gaylord, N. G.; Mehta, M. *J. Polym. Sci.: Polym. Lett. Ed.* **1982**, *20*, 481−486. Coutinho, F. M. B.; Ferreira, M. I. P. *Eur. Polym. J.* **1994**, *30*, 911−918. Gaylord, N. G.; Mishra, M. K. *J. Polym. Sci.: Polym. Lett. Ed.* **1983**, *21*, 23−30; de Roover, B.; Sclavons, M.; Carlier, V.; Devaux, J.; Legras, R.; Mourtaz, A. *J. Polym. Sci., Part A: Polym. Chem.* **1995**, *33*, 829−842. Heinen, W.; Rosemöller, C. H.; Wenzel, C. B.; de Groot, H. J. M.; Lugtenburg, J.; van Druin, M. *Macromolecules* **1996**, *29*, 1151−1157.

(15) Nemeth, S.; Jao, T.-C.; Fendler, J. H. *Photochem. Photobiol. A: Chem.* **1994**, *78*, 229−235.

(16) Liu, R.; Farinha, J. P. S.; Winnik, M. A. *Macromolecules* **1999**, *32*, 3957−3963.

(17) Walsh, E.; Gaymans, R. J. *Polymer* **1994**, *35*, 1774−1778.

(18) Demas, J. N. *Excited-State Lifetime Measurements*; Academic Press, New York, 1983; p 102.

(19) (a) Berlman, I. B. *Handbook of Fluorescence Spectra of Aromatic Molecules*; New York; Academic Press: 1971. (b) Measured on Pr. M. A. Winnik's (U. of Toronto, Canada) picosecond time-resolved fluorometer.

(20) Press, W. H.; Flannery, B. P.; Teukolsky, S. A.; Vetterling, W. T. *Numerical Recipes Fortran. The Art of Scientific Computing*; Cambridge University Press: New York, 1989; pp 523−528.

(21) Jones, A. S.; Dickson, T. J.; Wilson, B. E.; Duhamel, J. *Macromolecules* **1999**, *32*, 2956−2961.

(22) Lee, S.; Duhamel, J. *Macromolecules* **1998**, *31*, 9193−9200.

MA001211R